# ANODIC OXIDATION OF CUPROUS SULPHIDE IN AQUEOUS SOLUTIONS

by

MICHAEL J. FRASER

A THESIS SUBMITTED IN PARTIAL FULFILMENT OF
THE REQUIREMENTS FOR THE DEGREE OF
MASTER OF APPLIED SCIENCE

in the Department
of
METALLURGY

We accept this thesis as conforming to the required standard

Members of the Department of Metallurgy
THE UNIVERSITY OF BRITISH COLUMBIA

September 1965

In presenting this thesis in partial fulfilment of the requirements for an advanced degree at the University of British Columbia, I agree that the Library shall make it freely available for reference and study. I further agree that permission for extensive copying of this thesis for scholarly purposes may be granted by the Head of my Department or by his representatives. It is understood that copying or publication of this thesis for financial gain shall not be allowed without my written permission.

Department of Metallurgy

The University of British Columbia,
Vancouver 8, Canada

Date August 26, 1965

## ABSTRACT

The oxidation of artificial cuprous sulphide electrodes (Cu/S ratio = 1.93) was studied in acidified copper sulphate solutions in the temperature range 20 to 35° C. Rest potential measurements gave V° = 0.490 volts for the electrode or half cell potential. This is within the limits of accuracy of V° for:

$$Cu_2S \longrightarrow CuS + Cu^{++} + 2e \qquad V° = 0.535 \pm 0.13 \text{ volts}$$

The discrepancy was thought to be related to the large Cu deficiency in the sulphide. In solutions with pH>4, the rest potential measurements were consistent with the following reaction:

$$Cu_2S + 2H_2O \longrightarrow CuS + Cu(OH)_2 + 2H^+ + 2e$$

Polarization measurements at low overpotential gave values for the following kinetic parameters:

$\beta$, the symmetry factor = 1/2

$\lambda$, the number of electrons involved in each act of the rate determining step = 2

$i_o$, the exchange current $\approx 2 \times 10^{-5}$ A/cm$^2$

$\Delta H_o^*$, the standard heat of activation = 26.5 kcal/mole

CuS was tentatively identified as one of the reaction products. A reaction mechanism was discussed.

ACKNOWLEDGEMENT

I wish to thank Mrs. A. M. Armstrong for her assistance and constructive criticism during the work period and the thesis preparation.

A portion of the experimental work and the final preparation of the thesis were done in the Research and Development Department of The Steel Company of Canada, Limited, Hamilton. I wish to thank the following persons for their considerable assistance: J. C. McKay, Dr. W. G. Hines, Mrs. J. Cooke, C. E. Ohennesian, Miss P. A. Kriter and Mrs. M. Leedale.

TABLE OF CONTENTS

Table of Contents Continued

# LIST OF TABLES

List of Tables Continued

# LIST OF FIGURES

List of Figures Continued...

# INTRODUCTION

The oxidation of sulphide minerals to recover metals is accomplished on a commercial scale by both pyrometallurgical and hydrometallurgical methods, examples of which are suspension roasting, pressure leaching and anodic oxidation. Since 1954, the International Nickel Company of Canada, Limited, has produced nickel by a process in which cast nickel sulphide anodes are oxidized in electrolytic cells.[1,2,3] The success of this process indicated that attempts should be made to apply similar techniques to other sulphide minerals, so a preliminary study of the anodic oxidation of cuprous sulphide and tin sulphide was undertaken. The major portion of the study was devoted to cuprous sulphide and is reported in this thesis. A summary of the work carried out with tin sulphide is reported in Appendix A.

Cuprous sulphide is a compound semiconductor. The electrochemical behaviour of elemental semiconductor electrodes (e.g. Ge) differs from that of metallic electrodes because of differences in conductivity and conduction mechanisms, and because of the presence of a space charge layer in the solid at the solid-electrolyte interface. These same effects probably occur with compound semiconductor electrodes, but the background theory is not well-developed and experimental data are virtually non-existant. The following sections review both the present knowledge of the defect structures and conduction mechanisms in the Cu-S system, and some thermodynamic and kinetic aspects of the oxidation of cuprous sulphide.

## Physical Properties of Cuprous Sulphide

### The Copper Sulphur Binary System

The standard copper-sulphur binary system[44] is shown in Figure 1. A more detailed drawing of the $Cu_2S$-CuS portion of the binary, based on data from Hansen[44], Ruhl and Saur[42], Wagner[9], and Buerger[57], is shown in Figure 2. These figures reveal the three copper-sulphur compounds which have been identified: chalcocite or cuprous sulphide (approximately $Cu_2S$ with two allotropic forms - $\alpha$ and $\beta$); digenite (approximately $Cu_9S_5$); and covellite or cupric sulphide (approximately CuS).

The phase areas in Figure 2 are approximate only, because limited data are available on this portion of the binary. The $\alpha$ - $\beta$ transformation in $Cu_2S$ at 105°C is well established, and the point A on the $\beta$ $Cu_2S$-$Cu_9S_5$ boundary at 400°C was determined during electrochemical studies by Wagner and Wagner[9]. The existence of digenite has been amply confirmed[44], but the nature of the reaction or transformation occurring at 78°C is in doubt; the change is shown as the decomposition of digenite to form a mixture of chalcccite and covellite, but it may well be a transformation to an allotropic form.

The large miscibility gap and the limited solid solubility of sulphur in copper (0.0005 weight % at 600°C[44]) are not unusual features of sulphur-metal binary systems*.

---

* Binaries of S with Al, Sb, Cr, Cu, In, Mn, Pd, Ag, Tl and Sn have large immiscibility gaps; those with Bi, Co, Fe, Ni, Se, Te and V do not. The solid solubility of sulphur is extensive in Se (5-6 weight %) and Te (2-4 weight %), but very limited in all others.

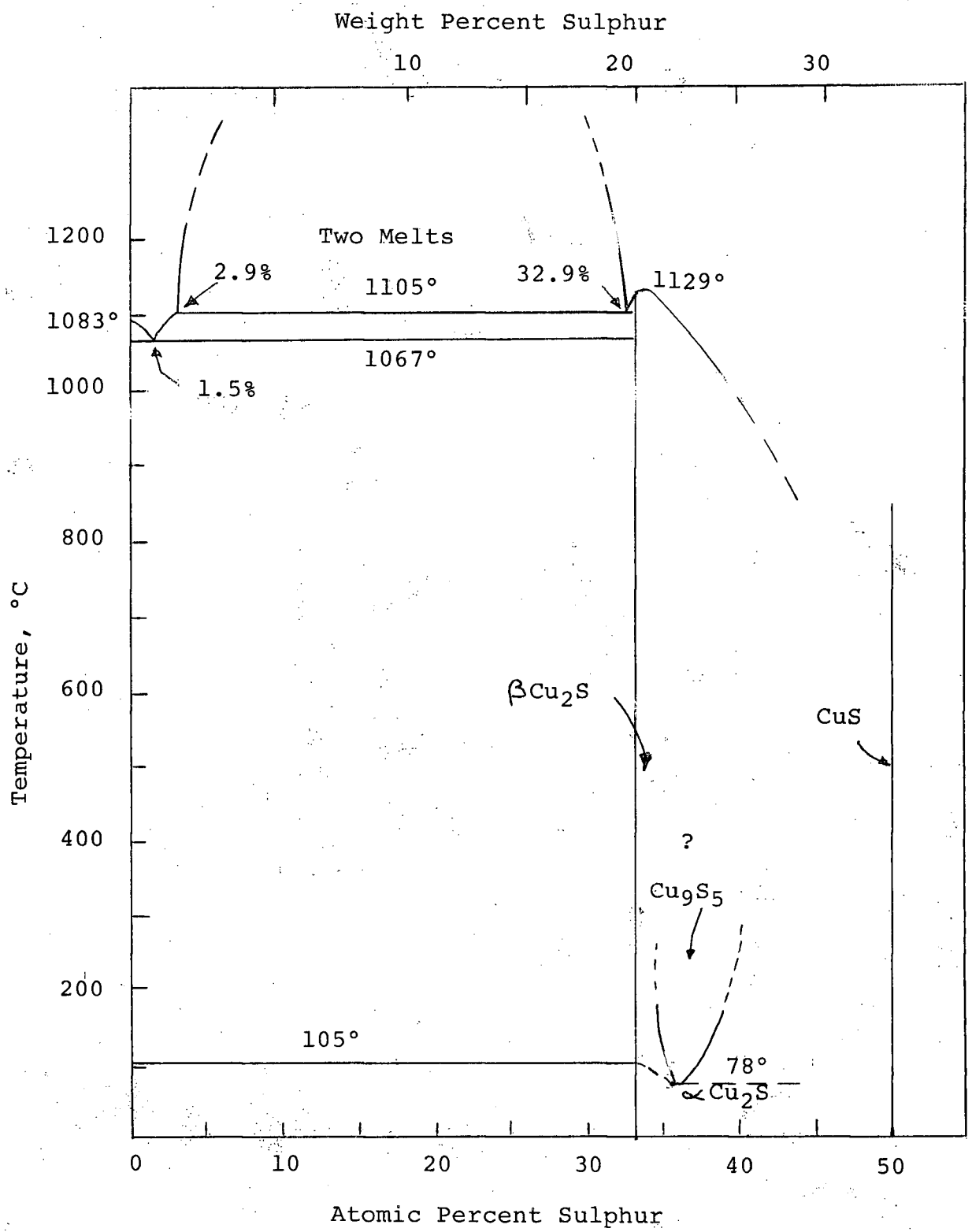


Figure 1. Copper-Sulphur Binary Diagram (After Hansen[44])

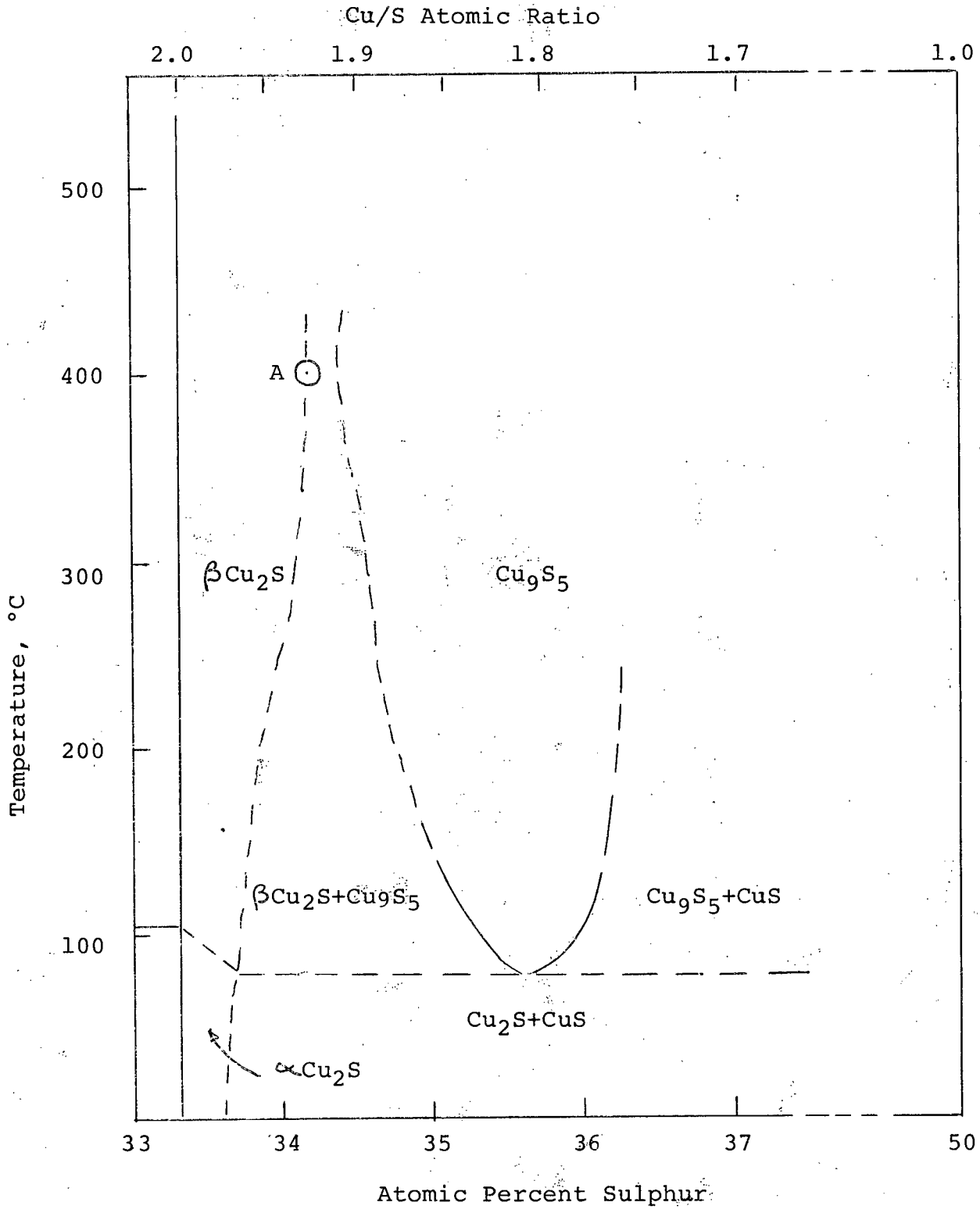


Figure 2. $Cu_2S$-CuS Portion of the Copper Sulphur Binary Diagram

## The Structure of the Copper Sulphides

The crystal structures of the three copper sulphides are summarized in Table I, as recorded by Hansen[44].

TABLE I

Copper Sulphide Crystal Structures

| | Chalcocite ∝ | Chalcocite β | Digenite | Covellite |
|---|---|---|---|---|
| Approximate composition | $Cu_2S$ | $Cu_2S$ | $Cu_9S_5$ | CuS |
| Class | orthorhombic | hexagonal | f.c.c. | hexagonal |
| Lattice Parameters | | | | |
| a Å | 11.90 | 3.89 | 5.575 | 3.75 |
| b Å | 27.28 | | | |
| c Å | 13.41 | 6.68 | | 16.2 |
| c/a | | 1.717 | | 4.32 |
| Atoms per unit cell | | 6 | | 12 |
| Formula weights per unit cell | 96 | | | |

Cuprous sulphide crystals consist essentially of monovalent copper ions and divalent sulphur ions. According to x-ray studies by Rahlfs[58], the copper ions are distributed virtually at random among a large number of nearly equivalent lattice sites, with the degree of randomness increasing with temperature. The sulphur ions appear to be quite highly ordered in the lattice[58,59]. Diffusion studies* indicate that the copper ions are quite mobile, while in contrast, the sulphur ions are virtually immobile.

In the case of cuprous sulphide deficient in copper (which appears to be the normal situation[9]), the charge balance

* see reference 9, p.1603

is maintained by the development of excess electrons and electron holes. The several species which exist in the cuprous sulphide are:

$Cu^{+}$: monovalent copper ion in a more or less random distribution.

$S^{=}$ divalent sulphur ion, in more or less regular lattice positions.

$Cu^{+\oplus}$: electron hole - a cuprous ion which has given up one electron i.e. a cupric ion.

$\ominus$ : excess electron - an unattached electron.

Powarennych[59] reviewed various crystallographic studies of the copper sulphides, and stated that the correct formulae of the various compounds are as follows:

| | |
|---|---|
| chalcocite | $Cu^{+}_{2}S$ |
| digenite | $Cu^{+}_{8}Cu^{+\oplus}S_{5}$ |
| covellite* | $Cu^{+}_{2}Cu^{+\oplus}S_{3}$ |

Conductivity of $Cu_2S$

Hirahara[62,63] measured the ionic and electronic conductivity of $Cu_2S$ at various temperatures, and his results are summarized in Table II.

---

* This formula for covellite requires the presence of a second sulphur species $S^{=}_{2}$ to maintain charge neutrality, viz:

$$(2Cu^{+})(Cu^{+\oplus})(S^{=})(S^{=}_{2})$$

TABLE II

Conductivity of $Cu_2S$

| Temperature °C | Ionic Conductivity $ohm^{-1}$ $cm^{-1}$ | Electronic Conductivity $ohm^{-1}$ $cm^{-1}$ |
|---|---|---|
| 25 | $\sim$ 0 | 55 |
| 100 | $\sim$ 0 | 62 |
| 150 | 0.0031 | 10 |
| 200 | 0.0144 | 13.1 |
| 300 | 0.089 | 14.6 |
| 400 | 0.20 | 15.7 |

It is concluded that ionic conductivity is of little significance below 150°C.

Wagner and Wagner[9] studied cuprous sulphide in a solid state cell

$$Cu \;|\; CuBr \;\|\; Cu_xS \;|\; \text{graphite} \qquad .....(1)$$

and found that the stoichiometry of the sulphide strongly influenced the conductivity. Some of their results at 400°C are summarized in Table III.

TABLE III

Electronic Conductivity of $Cu_xS$ at 400°C

| Cu/S Ratio | Cell Potential V | Electronic Conductivity $ohm^{-1}$ $cm^{-1}$ |
|---|---|---|
| 1.9996 | 0 | 0.3 |
| 1.9992 | 0.05 | 0.5 |
| 1.9975 | 0.10 | 6 |
| 1.9935 | 0.15 | 70 |
| 1.98 | 0.20 | 170 |

Their experiments also showed a strong dependence between the Cu/S ratio and the cell potential, and the following is a simplification of their interpretation. For $Cu_{2.000}S$, $x\theta^{\circ}$ and $(x\,Cu^{+\oplus})^{\circ}$ are the concentrations of excess electrons and cupric ions; Wagner and Wagner calculated

$$x\,\theta^{\circ} = (x\,Cu^{+\oplus})^{\circ} \leq 3.5 \times 10^{-4}/\text{per unit S} \quad .....(2)$$

If Cu is removed from the $Cu_xS$ by the following reactions:

$$Cu^{+}_{Cu_xS} \longrightarrow Cu^{+}_{CuBr} \quad .....(3)$$

$$\theta_{Cu_xS} \longrightarrow \theta_{graphite} \quad .....(4)$$

and the charge neutrality in the $Cu_xS$ is maintained by the following reaction:

$$Cu^{+}_{Cu_xS} \longrightarrow Cu^{+\oplus}_{Cu_xS} + \theta_{Cu_xS}, \quad .....(5)$$

then the net reaction is

$$2Cu^{+}_{Cu_xS} \longrightarrow Cu^{+\oplus}_{Cu_xS} + Cu^{+}_{CuBr} + \theta_{graphite} \quad .....(6)$$

Thus, as the Cu/S ratio in $Cu_xS$ drops, there is a net increase in the concentration of electron holes and no net increase in the concentration of excess electrons in $Cu_xS$. As the latter value is small to start with, the result is a corresponding decrease in the number of mutually annihilatory collisions between excess electrons and cupric ions, viz:

$$Cu^{+\oplus} + \theta \longrightarrow Cu^{+} \quad .....(7)$$

so the mobility of $Cu^{+\oplus}$ increases as well as the concentration. The conductivity is a function of both the mobility and concentration, so the conductivity of $Cu^{+\oplus}$, and in turn the cell potential, increase as the Cu/S ratio drops.

The influence of stoichiometry on cell potentials would probably be similar when a liquid electrolyte replaces the solid state CuBr electrolyte. No reference to this situation could be found.

## The Effect of Semiconductivity of Sulphides on their Electrochemical Behaviour

Semiconductors in general and compound semiconductors in particular differ from metals with respect to their potentials and potential distributions in two important ways:

(a) The electrochemical potential of electrons in a compound semiconductor can be varied over a wide range by the addition of suitable impurities* and, as previously noted, by changes in the stoichiometric ratio. For example: at 400°C, the electrochemical potential of Cu in cuprous sulphide changes by about 125 millivolts when the Cu/S ratio changes from 2 to 1.996[9]; and at room temperature, the electrochemical potential of the electrons in Ge changes by about 60 millivolts with the addition of $3 \times 10^{14}$ atoms/cc of As.

(b) The dielectric constant of most semiconductors is in the range of 10-20, while that of the metals approaches zero by definition. This factor, coupled with the lower free carrier density i.e. lower conduction electron concentration, enables semiconductors to support extensive space charges.

When a metal forms the two plates of a condenser, the potential is uniform throughout the bulk of each plate up to a position very near the surface, so the potential difference between the two plates is essentially the same as that between the surfaces of the two plates. However, when a semiconductor is made one plate of the condenser, a substantial portion of the

---

* Examples of suitable impurities: cations of different valence to normal cations, e.g. $Li^{+}$ and $Al^{+++}$ in NiO; and anions of different valence to normal anions, e.g. $Cl^{-}$ in $O^{=}$ lattice.

potential difference may occur within the semiconductor because the space charge has established a non-uniform potential distribution in the semiconductor. The internal space charge is equal but opposite in sign to the surface space charge.

The situation at the semiconductor-electrolyte interface is generally the same as that at a metal-electrolyte interface, with the exception of the added influence of the space charge. Usually, the space charge is only of significance in cases when the surface of the electrode has been preferentially concentrated with donor or acceptor atoms[15]. The space charge layer has a thickness of 100-10,000 Å in most semiconductors. The Helmholtz double layer (the region between the electrode and the plane of closest approach of ions in the electrolyte) is about 3 Å.

Thermodynamics of Oxidation of $Cu_2S$

The use of potential/pH diagrams to show the regions of thermodynamic stability of various species in aqueous solutions has been well developed, particularly by Pourbaix and his school[27,43]. Diagrams have been constructed for all the metal-water systems, and for a number of three-component systems. Horvath and Novak[48] published a diagram for the copper-sulphur-water system (Figure 3) which is useful in the study of the effect of S on the corrosion of Cu. They have simplified the system by ignoring all metastable sulphur-water forms, a simplification which appears necessary after examining the complexity of the sulphur-water binaries constructed by Valensi[28].

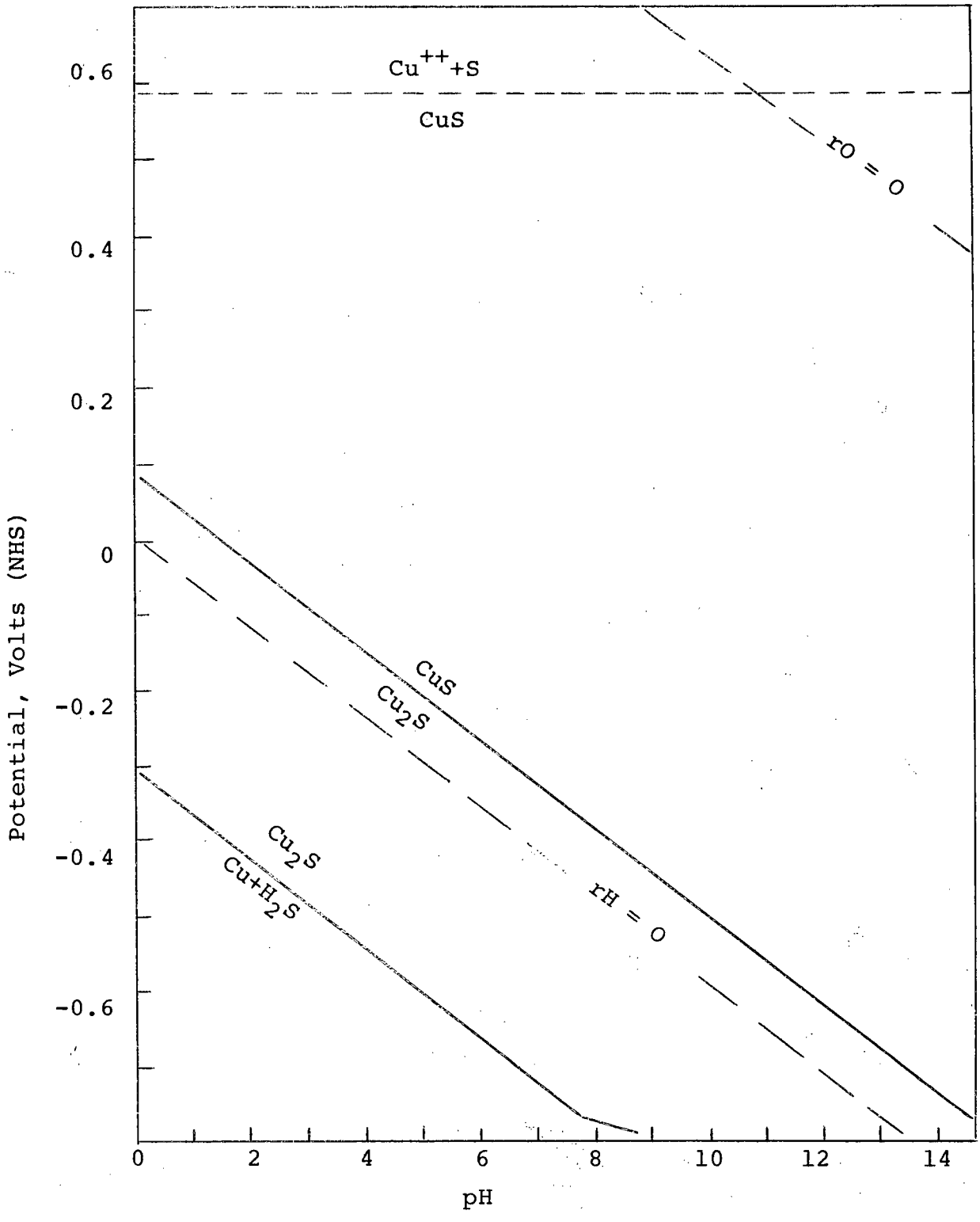


Figure 3. Potential/pH Diagram for the System $Cu-S-H_2O$ (after Horvath and Novak[48])

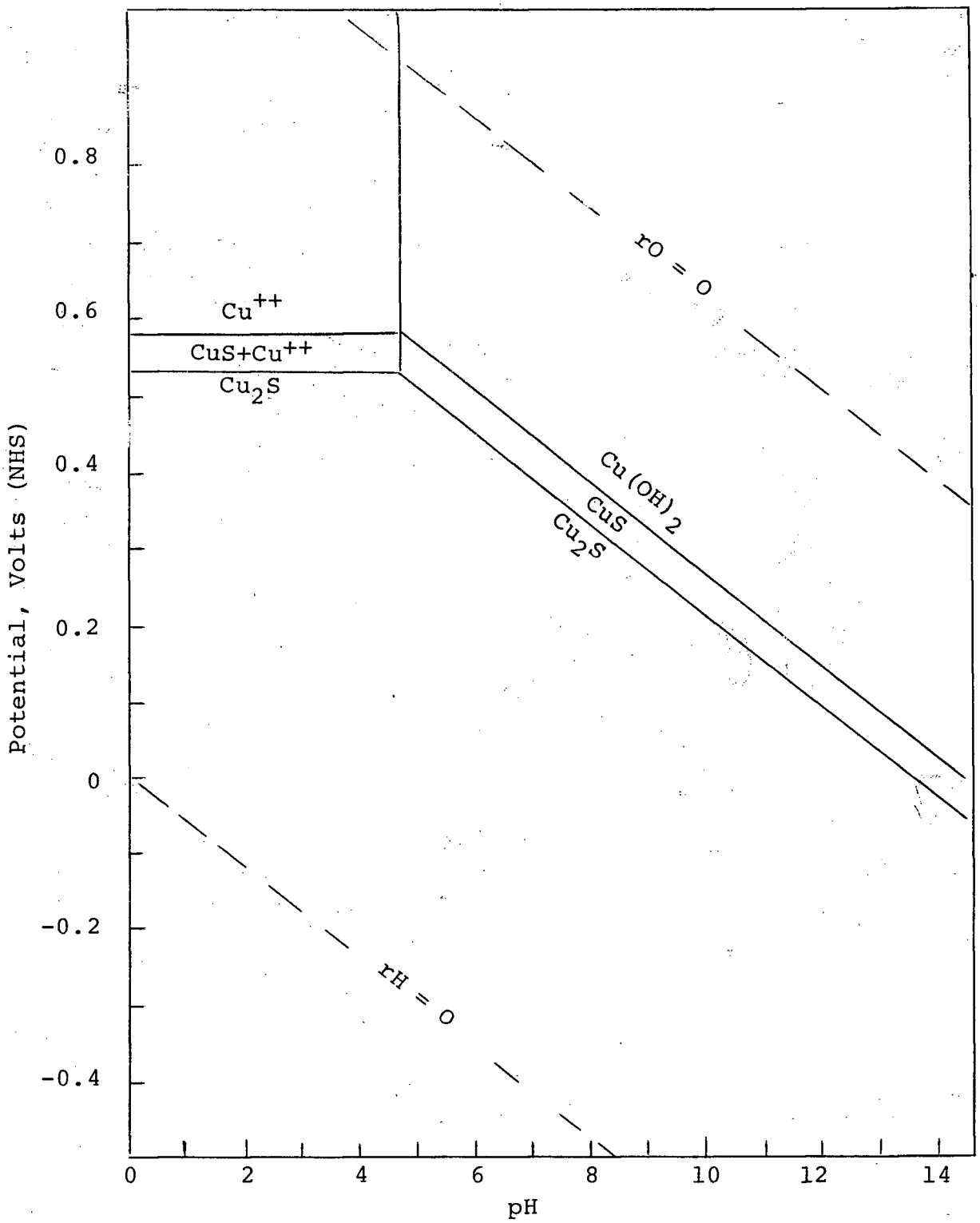


Figure 4. Potential/pH Diagram for the System Cu-S-$H_2O$, Omitting Oxidation Reactions with Metallic Cu. All species at Unit Activity.

A somewhat different diagram has been constructed (Figure 4) starting with $Cu_2S$ rather than Cu metal. No sulphur forms other than S are shown on the diagram, even though $SO_4^=$ is thermodynamically stable (see Table C-II, reactions 6 and 12). The $SO_4^=$ regions have been omitted because the reaction

$$S + 4H_2O \longrightarrow SO_4^= + 8H^+ + 6e^- \quad .....(8)$$

is extremely slow, and thus probably unimportant in the electrochemical oxidation of $Cu_2S$.

Chemical Oxidation of Cuprous Sulphide

Warren[49] studied the acid pressure leaching of three copper minerals - chalcopyrite, chalcocite and covellite - under the following conditions:

temperature: 100-200°C

pressure: 10-350 psi

acidity: 20-50 gpl $H_2SO_4$

$P_{O_2}$: 10-80 psi.

He concluded that a two-stage mechanism was operating in the oxidation of cuprous sulphide, implying that the reactions were:

$$Cu_2S + 1/2\ O_2 + 2H^+ \longrightarrow Cu^{++} + CuS + H_2O \quad .....(9)$$

$$CuS + 1/2\ O_2 + 2H^+ \longrightarrow Cu^{++} + S + H_2O \quad .....(10)$$

On the basis of reaction rate measurements, he calculated the activation energies of the rate-controlling steps of the two reactions to be 6.6 and 1.8 kcal/mole, respectively.

Sullivan[50] studied the oxidation of chalcocite by ferric sulphate in neutral and acid solutions at temperatures up to 50°C. He noted that little or no elemental sulphur was found

in the reaction products until approximately one-half of the copper in the cuprous sulphide had gone into solution. He concluded that the reaction proceeded in two steps:

$$Cu_2S + Fe_2(SO_4)_3 \longrightarrow CuSO_4 + 2FeSO_4 + CuS \quad \text{(fast)} \qquad .....(11)$$

$$CuS + Fe_2(SO_4)_3 \longrightarrow CuSO_4 + S + 2FeSO_4 \quad \text{(slow)} \qquad .....(12)$$

Electrochemical Oxidation of Cuprous Sulphide

Noddack and Wrabetz[11,12] and Sato[46,47] studied the behaviour of several sulphide electrodes, including cuprous and cupric sulphide, as part of geological investigations of sulphide ore bodies*. They noted that the rest potentials (i.e. open circuit potential) of the $Cu_2S$ and CuS electrodes were independent of pH and ($SO_4^=$) in acid solution, but were dependent on ($Cu^{++}$). Sato concluded that the potential-determining reactions were for the $Cu_2S$ and CuS electrodes respectively:

$$Cu_2S \longrightarrow CuS + Cu^{++} + 2e^- \qquad .....(13)$$

$$CuS \longrightarrow Cu^{++} + S + 2e^- \qquad .....(14)$$

Experimental values are compared in Table IV with those calculated from free energy data.

TABLE IV

Rest Potentials for $Cu_2S$ and CuS Electrodes at 25°C

| Electrode | Electrode Potential, V (NHS) | | |
|---|---|---|---|
| | Sato[47] | Noddack and Wrabetz[11,12] | Calculated |
| $Cu_2S$ | 0.504 | 0.47** | 0.535 (±0.13) |
| CuS | 0.567 | 0.58** | 0.588 (±0.13) |

* Their results are summarized and discussed briefly in Appendix D.

** Noddack and Wrabetz performed their experiments at temperatures other than 25°C, and usually at 18°C. The difference between

In basic solutions, the potential was a function of pH, presumably because of the hydrolysis of $Cu^{++}$, viz:

$$Cu^{++} + 2H_2O \rightleftharpoons Cu(OH)_2 + 2H^+ \quad .....(15)$$

The resulting overall reactions are, for the $Cu_2S$ and CuS electrodes respectively:

$$Cu_2S + 2H_2O \rightarrow CuS + Cu(OH)_2 + 2H^+ + 2e^- \quad .....(16)$$

$$V = 0.802 - 0.0591\ pH$$

$$CuS + 2H_2O \rightarrow Cu(OH)_2 + S^\circ + 2H^+ + 2e^- \quad .....(17)$$

$$V = 0.862 - 0.0591\ pH.$$

Sato suggested that the potential-determining reaction for the $Cu_2S$ electrode may involve digenite:

$$5Cu_2S \longrightarrow Cu^{++} + Cu_9S_5 + 2e^- \quad .....(a)$$

$$Cu_9S_5 \longrightarrow 5CuS + 4Cu^{++} + 8e^- \quad .....(b) \quad (18)$$

$$CuS \longrightarrow Cu^{++} + S + 2e^- \quad .....(c)$$

He postulated that the 0.031 V difference between his experimental value and the calculated value of the electrode potential (Table IV) might be due to reactions (18 a) or (18 b) being potential-determining. However, the accuracy of the thermodynamic data from which the electrode potentials were calculated is such that a difference of 0.031 V is not unreasonable (see Tables IV and C-II). Furthermore, stoichiometric deviations have a significant effect on the electrode potential; Sato did not report the analysis of his electrode, but it may have had a large Cu deficiency which could have altered the electrode potential. No

---

(cont'd from p.14) $V^\circ$, the electrode potential, calculated at 18 and 25°C would only be about 0.005 V for most electrodes[60], so no correction has been made.

thermodynamic data are available for digenite. It would appear, then, that direct observation of the reaction products is necessary to resolve the nature of the potential-determining reaction unequivocally.

During their study of the oxidation of nickel sulphide electrodes, Renzoni et al[1] briefly examined the oxidation of cuprous sulphide, and suggested that the mechanism involved the following steps:

$$Cu_2S \longrightarrow Cu^+ + CuS + e^- \quad .....(a)$$
$$Cu^+ \longrightarrow Cu^{++} + e^- \quad .....(b) \quad (19)$$
$$CuS \longrightarrow Cu^{++} + S + 2e \quad .....(c)$$

However, no rest potential measurements were reported. Their identification of CuS as an intermediate reaction product appears plausible, but no support is given for their selection of $Cu^+$ as the initial aqueous ion. The final reaction products were stated to be $Cu^{++}$ and S.

Aylen[61] determined the rest potential of a $Cu_2S$ electrode to be 0.477 V in acid copper sulphate solution at 25°C.

When they oxidized the nickel sulphide and copper sulphide anodes, Renzoni et al[1] noted that the nickel and copper dissolved in the electrolyte solution leaving an essentially intact structure of sulphur, an observation which is consistent with the sulphide structure described earlier (i.e. stable sulphur lattice, mobile Cu atoms). In the commercial nickel sulphide process, the anodes are placed in porous bags during

electrolysis to prevent the contamination of the electrolyte with sulphur. A number of metals, particularly selenium, remain with the sulphur sludge and are recovered in a subsequent process.

General Discussion of Electrode Kinetics

The rates of electrode reactions can most conveniently be followed by measuring the current density as a function of the electrode potential. The resulting relationship, when plotted, is called a polarization curve. If it is possible to minimize extraneous diffusion and ohmic effects (see Appendix D), then the polarization curves can be analysed to aid in determining the electrode reaction mechanism.

In Appendix E, a derivation of several important polarization relationships is presented. Two of these are stated below:

for an activation-controlled reaction, when

$$\omega > \frac{2.303\ RT}{\lambda 7} \quad (\text{i.e. } \omega > \sim 20 \text{ mV})$$

then

$$\ln i_A = \ln i_0 + \frac{(1-\beta)\lambda 7\, \omega}{RT} \qquad .....(20)$$

for an activation-controlled reaction, when

$$\omega < \frac{2.303\ RT}{\lambda 7} \quad (\text{i.e. } \omega < \sim 20 \text{ mV})$$

then

$$i_A = i_0\ \frac{\lambda 7}{RT}\ \omega \qquad .....(21)$$

where

$\omega$ = Overpotential

$i_A$ = Net anodic current density

$i_0$ = Exchange current

$\beta$ = Activation barrier symmetry factor

$\lambda$ = Stoichiometric factor

$\mathcal{F}$ = Faraday constant

R = Gas constant

T = Absolute temperature

In the rest state, a potential is developed at the electrode-solution interface which is consistent with the chemistry of the two phases, solid and solution. Although there is almost certainly a flow of electrical charges in both directions across the anode-solution interface in the rest state, there is no net flow in one or other direction; i.e. the current is the same in both directions, thus maintaining the electrical neutrality of the system. The current density in both directions across the solution-solid interface in the rest state is called the exchange current*. Table V lists values of the exchange current for various electrochemical reaction; the data for anodic dissolution of metals or compounds are very meagre. A simple description of the exchange current is that it is a measure of the relative ability of the electrode to take part in the particular electrode reaction. For the case of hydrogen evolution on metal cathodes, Bockris[14] has pointed out that there is a strong relationship between $i_0$, the exchange current, and $\phi$, the thermionic work function, where $\phi$ is a measure of the ease with which electrons leave the metal; the greater $\phi$, the greater $i_0$.

---

* For heterogeneous reactions, the current will be equivalent to an apparent current density.

TABLE V

Values of the Exchange Current for Various Electrochemical Reactions

| Situation | Exchange Current $i_0$ A/cm$^2$ at 25°C | Reference |
|---|---|---|
| Metal Dissolution: | | |
| $Cu/Cu^{++}$ in 1 M $CuSO_4$* | $1 - 2 \times 10^{-3}$ | 32 |
| $Fe/Fe^{++}$ in 1 M $FeSO_4$ | $(OH^-)$ dependent | 33 |
| Metal Deposition: | | |
| Cu on Cu from 1 M $CuSO_4$* | $2 \times 10^{-5}$ | 14 |
| Fe on Fe from 1 M $FeSO_4$ | $10^{-8}$ | 14 |
| Hydrogen Evolution: | | |
| on Au in 1.0 N Hcl | $10^{-5} - 10^{-6}$ | 14 |
| Cd in 1.0 N Hcl | $10^{-7}$ | 14 |
| Hg in 0.1 N Hcl | $5 \times 10^{-13}$ | 14 |
| Pb in 0.1 N Hcl | $2 \times 10^{-13}$ | 14 |
| Pt in 1.0 N Hcl | $10^{-3}$ | 14 |
| Oxygen Evolution: | | |
| on Pt in 0.1 N $H_2SO_4$ | $2 \times 10^{-10}$ | 14 |
| $Fe^{++} - Fe^{+++}$ redox system in sulphate solution on Type 304 Stainless Steel | $4.5 \times 10^{-8}$ | 21 |

* These results are anomalous; the $i_0$ values should be the same for the same concentration of $Cu^{++}$, all other factors being equal.

The symmetry factor, $\beta$, indicates the portion of the overpotential which is actually operating between the initial point of the reaction and the peak of the energy barrier existing between the initial and final state. This is the important region along the reaction path, for once a reacting species passes over the peak of the energy barrier, it requires no further driving force to reach the final state. Although it is convenient to think of the energy barrier as having a physical shape, this is not necessary for a formal development of the rate expressions;

the term $\beta$ can be considered to be only a mathematical convenience, a number between 0 and 1. Quite often, $\beta$ has the value of 1/2 and in these cases, the energy barrier, regardless of the interpretation of its physical shape, is truly symmetrical.

The stoichiometric factor $\lambda$ is a two-component factor:

$$\lambda = n/\nu \qquad .....(22)$$

where n is the number of electrons involved in the overall electrode process, and $\nu$ is the number of times the rate determining step occurs while the overall reaction occurs once. Then $\lambda$ is the number of electrons involved in one act of the rate determining step. If reasonable data are available and can be treated by the mathematical methods described above, some information on the nature of the electrochemical reactions should be revealed upon determination of the parameters $\lambda$, n, $\beta$ and $\nu$. Such data can be used further in some cases to give the heat of activation. Hurlen[34,35] developed a formula for determining the standard heat of activation, $\Delta H_o^*$, for reactions where $\beta = 0.5$, viz:

$$\Delta H_o^* = 2.303\ R\ \frac{d \log (J_o/T)}{d\ (1/T)} + \frac{1}{2\nu}\ \Delta H_o \qquad .....(23)$$

where

$\Delta H_o^*$ = Standard heat of activation

R = Gas constant

$J_o$ = Standard exchange current density (see Appendix F)

T = Absolute temperature

$\Delta H_o$ = Standard heat of reaction

Object and Scope of Present Work

Cuprous sulphide electrodes were prepared and both rest potential and polarization measurements were obtained in various solutions.

The rest potential measurements have been analysed to provide a value for the electrode potential $V^\circ$ for cuprous sulphide, and the discrepancies between this value, that calculated from free energy data, and that determined by Sato have been discussed.

Most of the polarization measurements were made at low values of the overpotential between 20 and 35°C as this region provided the only reproducible results. Certain kinetic parameters were calculated.

The results are reviewed in terms of possible reaction mechanisms, and the additional data required to differentiate between the several possibilities are discussed.

# APPARATUS AND EXPERIMENTAL PROCEDURES

## The Electrolytic Cell

The electrolytic cell used in this work (Figure 5) consisted of a 4-liter pyrex beaker with a close fitting lid and contained three electrodes - anode, cathode, and reference -, a glass stirring rod driven by a variable speed motor, a gas inlet and a thermometer (range: -1 to +101°C in divisions of 0.1°C). The cell was placed in a 20 liter water bath heated by an electric coil and cooled when necessary by either tap water in a copper coil or ice cubes. The temperature was controlled within $\pm 0.1$°C by a Philadelphia Microset Controller in series with a Merc-to-Merc relay switch.

A nitrogen atmosphere was usually maintained in the cell to minimize oxidation by $O_2$. Commercial grade $N_2$ was purified by passage through a chromous sulphate solution.

## Measuring Circuit

A simple potential- and current-measuring circuit (Figure 6) was used. Potentials were impressed across the anode and cathode using three 2V lead-acid batteries in series and a slide wire rheostat as a potential divider. The potentials between the various electrodes were measured by a Pye potentiometer and an auxiliary mirror galvanometer. The potentiometer had three ranges - 0-0.01799 V, 0-0.1799 V and 0-1.799 V. Currents up to one mA were measured with an RCA ultra-sensitive DC micro-ammeter (full-scale movement = 0.5 V); after calibration with the potentiometer, the

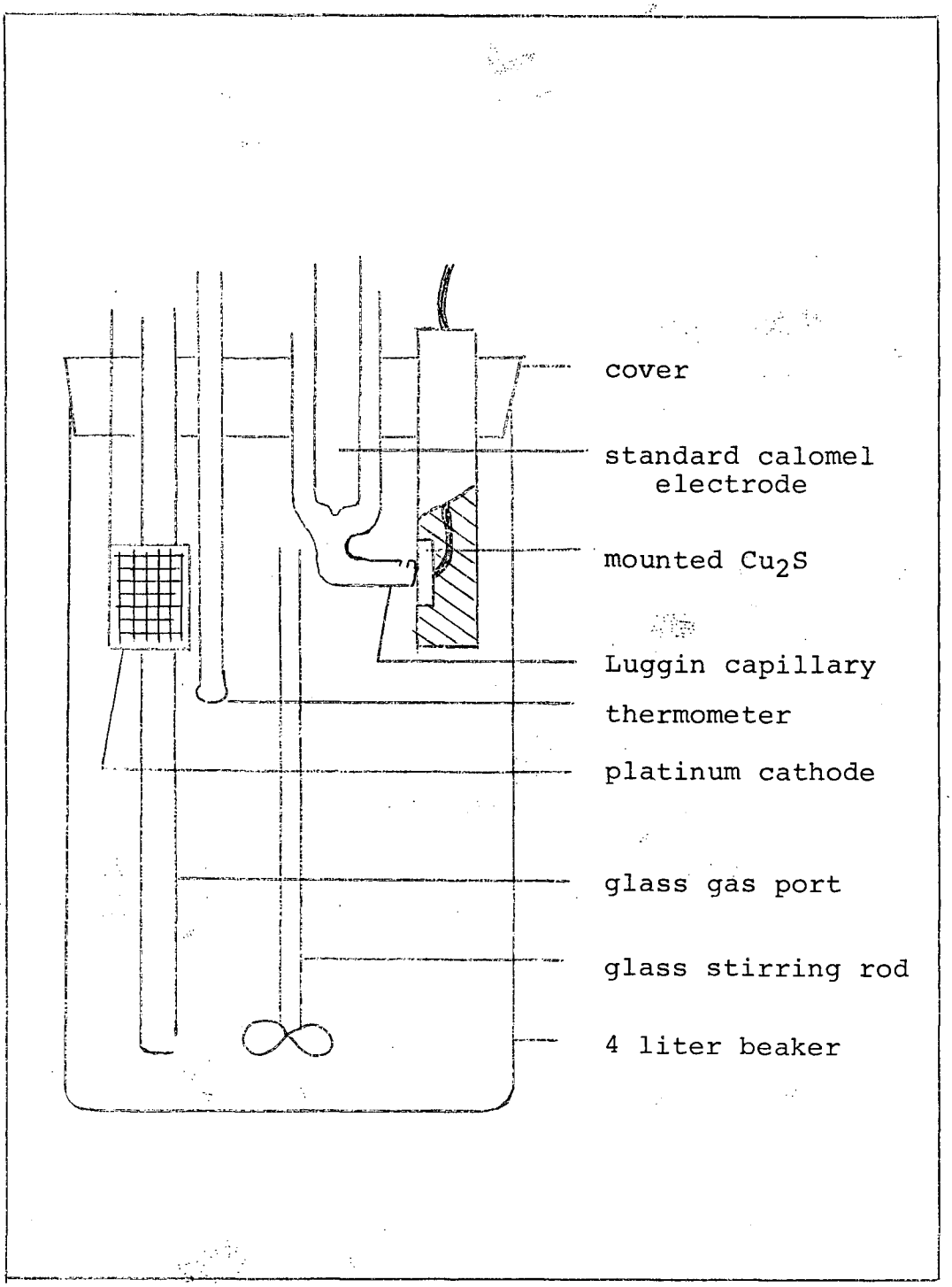


Figure 5. Cell for Potential Measurements

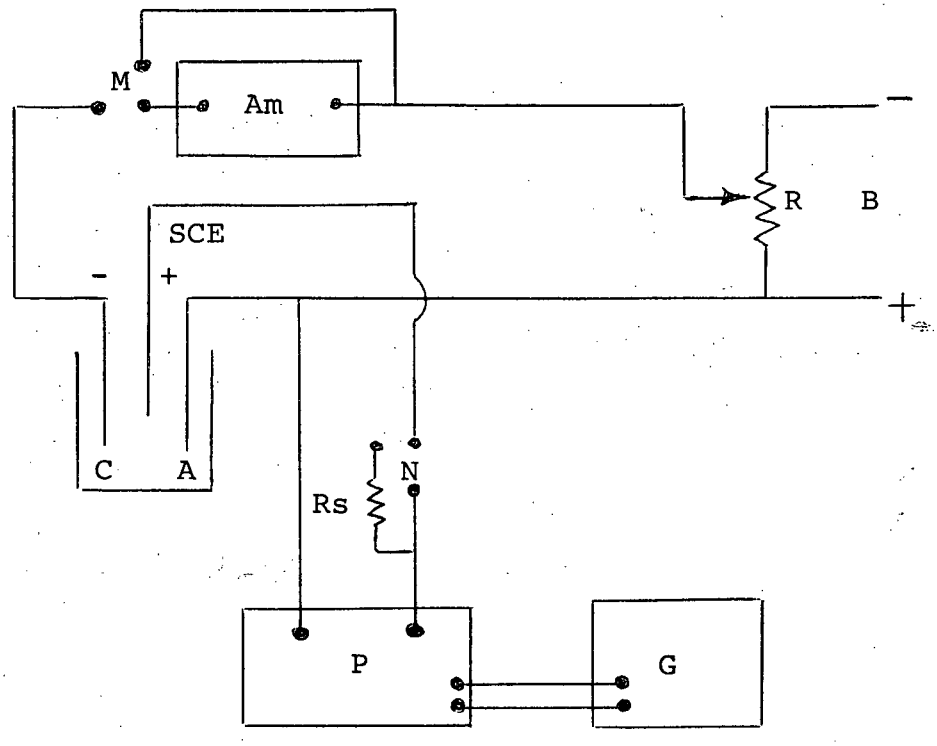


| | | | | | |
|---|---|---|---|---|---|
| P | = | potentiometer | Rs | = | safety resistance |
| G | = | galvonometer | SCE | = | reference electrode |
| Am | = | ammeter | C | = | cathode |
| B | = | power supply | A | = | anode |
| R | = | rheostat | M, N | = | switches |

Figure 6. Circuit for Potential and Current Measurements

accuracy of the unit was about ±2% of the full-scale reading. Currents above one mA were measured with a Heathkit Multimeter with an accuracy of about ±2% of the full-scale reading (most measurements were taken on the 150 mA range, so the accuracy in this case was about ±3 mA).

Anodes

The cuprous sulphide anodes were prepared by direct combination of copper and sulphur in a clay crucible at 400°C. The resulting sulphide was placed in a graphite crucible, melted in a gas-fired furnace at about 1130°C and cast into 1/2" x 3/8" x 2" pieces. After solidifying, the sulphide was held at about 100°C for one hour to prevent cracking due to rapid cooling through crystallographic transformation temperatures. The material was analysed to determine the stoichiometry.

A piece of silver foil was cut to fit one side of the cast sulphide and a length of copper wire was soldered to the silver. The silver foil was pressed firmly against the sulphide surface and the combination was mounted in Moldpac* so that only one surface of the sulphide remained exposed. This surface was polished by standard metallographic techniques (Figure 7) and then placed immediately in the electrolytic cell.

---

* "Moldpac" is a repair acrylic (manufacturer: Motloid Company, Chicago, Ill.) which is virtually insoluble in acid solutions.

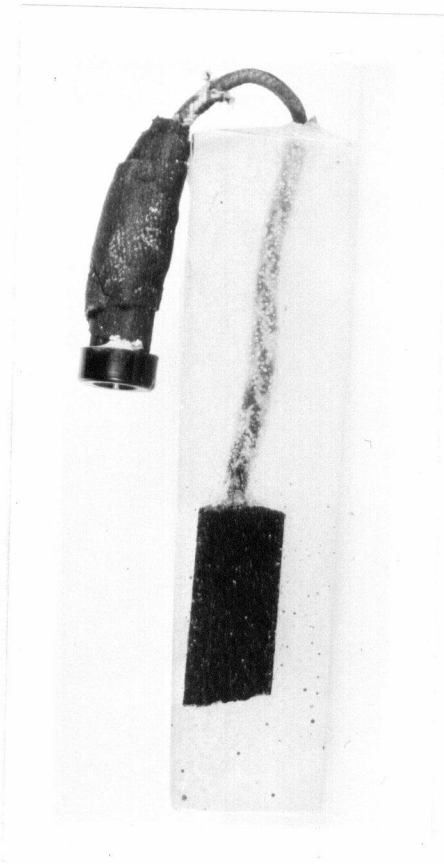

Figure 7. Mounted Copper Sulphide Electrode

Other Electrodes

The cathode of the working cell was either a standard analytical platinum gauze electrode or a plate of copper. The reference electrode was a Beckman standard saturated calomel electrode mounted in a Luggin capillary tube. The construction of the latter was based on the design proposed by Piontelli[23], a design which allows the reference electrode to be in contact with the solution immediately adjacent to the anode (see Figure 5). The potentials exerted by the reference electrode at several temperatures are shown in Table VI, as calculated from the following half-cell relationship[17]:

Hg, $Hg_2cl_2$(S), saturated Kcl

$$\mathcal{E} = -0.2415 + 0.00076(t - 25) \qquad .....(24)$$

TABLE VI

The Potential of the Saturated Calomel Electrode

| Temperature, °C | Oxidation Potential $\mathcal{E}$, volts (NHS) | Electrode Potential V, volts (NHS) |
|---|---|---|
| 20 | -0.2453 | 0.2453 |
| 25 | -0.2415 | 0.2415 |
| 30 | -0.2377 | 0.2377 |
| 35 | -0.2339 | 0.2339 |

Solutions

Stock solutions of $CuSO_4$, $H_2SO_4$, $MgSO_4$, $NaHSO_4$ and $HclO_4$ were prepared from either reagent grade chemicals or known standards, analysed, and diluted with distilled water to provide experimental

solutions of the required concentration. The following analytical techniques were used: for $Cu^{++}$, electrolytic recovery of Cu; for $H^{+}$, potentiometric titration with boric acid; and for S, the Eschka procedure[64].

Rest Potential Measurements

The test solution was prepared and allowed to come to the desired temperature under stirred conditions. Nitrogen was passed through it for several hours before the electrode was inserted. After being polished and cleaned with ethanol, the electrode was inserted and the Luggin capillary adjusted to be in immediate contact with the electrode surface.

Potential measurements were made intermittently over a period of hours. In the early tests, potentials were measured for a period of 40-50 hours, but as the readings were very consistent, later measurements were terminated after a period of 10-20 hours.

The electrodes were connected to the measuring potentiometer only at the time of measurement to minimize the opportunity for stray currents from various sources to act on the electrode.

Polarization Measurements

The electrode and solution were prepared as before. The applied potential was varied incrementally by use of the slide wire rheostat, and the electrode potential and cell current were

measured. With overpotentials of up to 50-100 mV, the readings were very stable; at higher overpotentials considerable variation was noted. At low overpotentials, a time of about 1 minute was allowed at each potential setting to determine if there was any noticeable fluctuation. If no fluctuation was noted, the potential was then increased; if a fluctuation was noted, it was followed for several minutes or until a steady condition was attained.

At the conclusion of some of the polarization runs, the surface of the electrode was observed under the microscope, and a portion of the corroded electrode was analysed chemically and studied by x-ray methods.

# RESULTS AND DISCUSSION

## Analysis of $Cu_2S$

Chemical analysis of the cuprous sulphide gave the following results:

Cu = 78.5 $\pm$0.2 wgt. %

S = 20.5 $\pm$0.4 wgt. %

Atomic ratio, Cu/S = 1.93

This analysis indicates that the electrode is cuprous sulphide with a large copper deficiency. The Cu/S ratio of 1.93 places the material in either the $\beta$ $Cu_2S$ + digenite region or the $\alpha$ $Cu_2S$ + CuS region of the Cu-S system (Figure 2), depending on the temperature. An x-ray powder pattern was obtained and its analysis (Appendix H) suggests that the electrode is chalcocite.

## Rest Potential Measurements

Rest potential measurements were made with several electrodes. It was previously noted that silver foil had been used at the electrode-connecting wire junction in order to minimize the contact potential, but when rest potential measurements were made with two electrodes, one with the silver foil and one without, little variation was observed (see Table VII).

The nitrogen was necessary in the electrolytic cell in order to obtain consistent results. For example, when $N_2$ was turned off overnight in one rest potential measurement, the potential rose from about 0.2 to about 0.4 V. When nitrogen was used, the potential remained constant for long periods (up to 50 hours).

TABLE VII

Electrode Potential of Cuprous Sulphide Anodes, With and Without Silver Foil Contact

| Solutions* | Electrode Potential w.r.t. Reference Electrode, V | |
|---|---|---|
| | With silver foil | Without silver foil |
| 0.01 M $CuSO_4$ | -0.171 | -0.172 |
| 0.1 M $CuSO_4$ | -0.195 | -0.194 |
| 0.77 M $CuSO_4$ | -0.215 | -0.215 |
| 0.77 M $CuSO_4$ 0.5 M $Na_2SO_4$ | -0.211 | -0.211 |

* Solution Analysis approximate only.

Rest potentials were measured in $CuSO_4$ at several levels of concentration. Using the activity coefficients measured by Robinson and Jones[16], values of the electrode potential, $V°_{Cu_xS}$, have been calculated (Table VIII) using the relationship

$$\mathcal{E}_{cell} = V_{S.C.E.} - V_{Cu_xS}$$

$$= V_{S.C.E.} - (V°_{Cu_xS} + \frac{RT}{n\mathcal{F}} \ln a_{Cu^{++}}) \quad .....(25)$$

where $\mathcal{E}_{cell}$ is the measured potential and n is assumed to equal 2. The calculations give $V°_{Cu_xS} = 0.490 \pm 0.002$ V at 25°C.

Measurements made in $CuSO_4$-$MgSO_4$-$H_2SO_4$ solutions of constant ionic strength have been interpreted in two ways:

(a) Using $V°_{Cu_xS} = 0.490$ V, values of $\gamma_{Cu^{++}}$ were calculated (Table IX). These values ranged from 0.077 to 0.104.

(b) Using $\gamma_{Cu^{++}} = 0.1$ (see Appendix G) and assuming $\gamma_{Cu^{++}}$ remains constant in solutions of constant ionic strength, despite changes in molarity, values of $V°_{Cu_xS}$ were calculated

(Table X). These values ranged from 0.487 to 0.491 V.

TABLE VIII

Electrode Potential $V°_{Cu_xS}$ in $CuSO_4$ at 25°C

| Run No. | $\mathcal{E}_{cell}$, V | $M_{Cu^{++}}$ | $m_{Cu^{++}}$* | $\gamma_{Cu^{++}}$ (Ref. 16) | $\frac{RT}{n\mathcal{F}} \log a_{Cu^{++}}$ V | $V°_{Cu_xS}$, V |
|---|---|---|---|---|---|---|
| SM 1 | -0.205 | 0.559 | 0.562 | 0.058 | -0.0439 | 0.490 |
| SM 2 | -0.213 | 1.665 | 1.923 | 0.0345 | -0.0348 | 0.489 |
| SM 3 | -0.2015 | 0.273 | 0.274 | 0.087 | -0.0479 | 0.492 |
| SM4 | -0.197 | 0.158 | 0.159 | 0.118 | -0.0510 | 0.489 |

* moles/1000 gm water

TABLE IX

$\gamma_{Cu^{++}}$ in $CuSO_4$-$MgSO_4$-$H_2SO_4$ Solutions of Constant Ionic Strenght at 25°C

| Run No. | $\mathcal{E}_{cell}$, V | Concentration*, M $CuSO_4$ | $MgSO_4$ | $H_2SO_4$ | $\frac{RT}{n\mathcal{F}} \log a_{Cu^{++}}$ V | $a_{Cu^{++}} \times 10^5$ | $\gamma_{Cu^{++}}$ |
|---|---|---|---|---|---|---|---|
| SF 1 | -0.186 | 0.100 | 0 | 0.100 | -0.0625 | 768 | 0.077 |
| SF 2 | -0.1585 | 0.010 | 0.090 | 0.100 | -0.0900 | 90.1 | 0.090 |
| SF 3 | -0.130 | 0.001 | 0.099 | 0.100 | -0.1185 | 9.76 | 0.098 |
| SF 4 | -0.1103 | 0.0002 | 0.0999 | 0.100 | -0.1382 | 2.09 | 0.104 |

* molarity $\approx$ molality at these concentrations.

Some support for the latter assumption is given by Lewis and Randall[18,40], who state that for a single electrolyte in solution, the following relationship holds for dilute solutions i.e. generally under 0.01 M

$$\log \gamma = -A \left| Z_+ Z_- \right| \mu^{0.5} \quad \ldots\ldots(26)$$

where $Z_+$ and $Z_-$ are the electronic charges of the positive and negative ions and A is a constant for a particular solvent at a particular temperature. Then if $\mu$ remains constant and $Z_+$ and $Z_-$ remain constant, $\gamma$ should remain constant. The uniformity of the values of $V°_{Cu_xS}$ calculated by this method suggests that the values of $\gamma_{Cu^{++}}$ obtained from electromotive force measurements by the method of Argersinger[25] (Appendix G) have some validity. However more extensive test work than was undertaken here would be required to confirm this point.

TABLE X

$V°_{Cu_xS}$ in $CuSO_4$-$MgSO_4$-$H_2SO_4$ Solutions of Constant Ionic Strength at 25°C

| Run No. | $\mathcal{E}_{cell}$, V | Concentrations, M $CuSO_4$ | $MgSO_4$ | $H_2SO_4$ | $a_{Cu^{++}}$ ($\gamma_{Cu^{++}} = 0.1$) | $\frac{RT}{n\mathcal{F}} \log a_{Cu^{++}}$ V | $V°_{Cu_xS}$, V |
|---|---|---|---|---|---|---|---|
| SF 1 | -0.186 | 0.100 | 0 | 0.100 | 0.01 | -0.0591 | 0.487 |
| SF 2 | -0.1585 | 0.010 | 0.090 | 0.100 | 0.001 | -0.0886 | 0.489 |
| SF 3 | -0.130 | 0.001 | 0.099 | 0.100 | 0.0001 | -0.1182 | 0.490 |
| SF 4 | -0.1103 | 0.0002 | 0.0999 | 0.100 | 0.00002 | -0.1398 | 0.491 |

The cell potential was measured in $CuSO_4$-$H_2SO_4$-$NaHSO_4$ solutions of constant $Cu^{++}$ concentration and varying $H_2SO_4$ concentration. The $NaHSO_4$ was added in an attempt to maintain the ionic strength at a constant value. The ionic strength probably did not remain constant, however, because of further dissociation of $HSO_4^-$*. Values of ionic strength are calculated in Table XI

* For $HSO_4^- \rightleftharpoons H^+ + SO_4^=$,

$K_{dis.} = 1.26 \times 10^{-2}$, according to Latimer[19].

TABLE XI

Rest Potential Measurements in $CuSO_4$-$H_2SO_4$-$NaHSO_4$ Solutions at 25°C

| | Molarity | | | Concentration at Equilibrium | | | Ionic Strength Δ | pH (measured) | Cell Potential, V |
|---|---|---|---|---|---|---|---|---|---|
| | $CuSO_4$ | $H_2SO_4$ | $NaHSO_4$ | $SO_4^{=}$ | $HSO_4^{-}$ | $H^{+}$ | | | |
| SF 1 | 0.100 | 0.100 | - | 0.045 | 0.155 | 0.045 | 0.390 | - | -0.186 |
| SF 5 | 0.100 | 0.050 | 0.050 | 0.072 | 0.128 | 0.022 | 0.444 | 1.45 | -0.185 |
| SF 6 | 0.100 | 0.010 | 0.090 | 0.102 | 0.098 | 0.012 | 0.504 | 1.5 | -0.184 |
| SF 8 | 0.100 | 0.001 | 0.099 | 0.109 | 0.101 | 0.010 | 0.523 | 1.75 | -0.184 |

Δ Calculated from equilibrium concentrations.

assuming equilibrium dissociation of $HSO_4^-$. Because of the apparent variation of the ionic strength, the same value of $\gamma_{Cu^{++}}$ cannot be used in all cases, so no attempt has been made to calculate values of $V°_{Cu_xS}$. The constancy of the measured cell potential indicates that there is little or no variation with pH, at least in the range pH=1-2.

A few rest potentials were measured in buffered solutions at higher pH, using the McIlvaine's standard buffer solutions[24] up to pH = 8 and a 0.1 molar sodium bicarbonate-sodium carbonate buffer at pH = 10.5. They are shown in Figure 8 and compared with similar results obtained by Sato[47]. The agreement is reasonable with the calculated line for the reaction:

$$Cu_2S + 2H_2O \rightarrow CuS + Cu(OH)_2 + 2H^+ + 2e^- \quad .....(27)$$

In summary, the rest potential measurements appear to be consistent with the following potential determining reactions: at pH < 4

$$Cu_2S \longrightarrow CuS + Cu^{++} + 2e^- \quad .....(28)$$

at pH > 4

$$Cu_2S + 2H_2O \longrightarrow CuS + Cu(OH)_2 + 2H^+ + 2e^- \quad .....(29)$$

The experimentally determined value of $V°_{Cu_2S}$ is 0.490 V, which can be compared with the calculated value of 0.535 V. The discrepancy is actually within the possible error of $\pm$0.13 V for the calculated value, but it may also be a function of the quite large Cu deficiency in the experimental electrode.

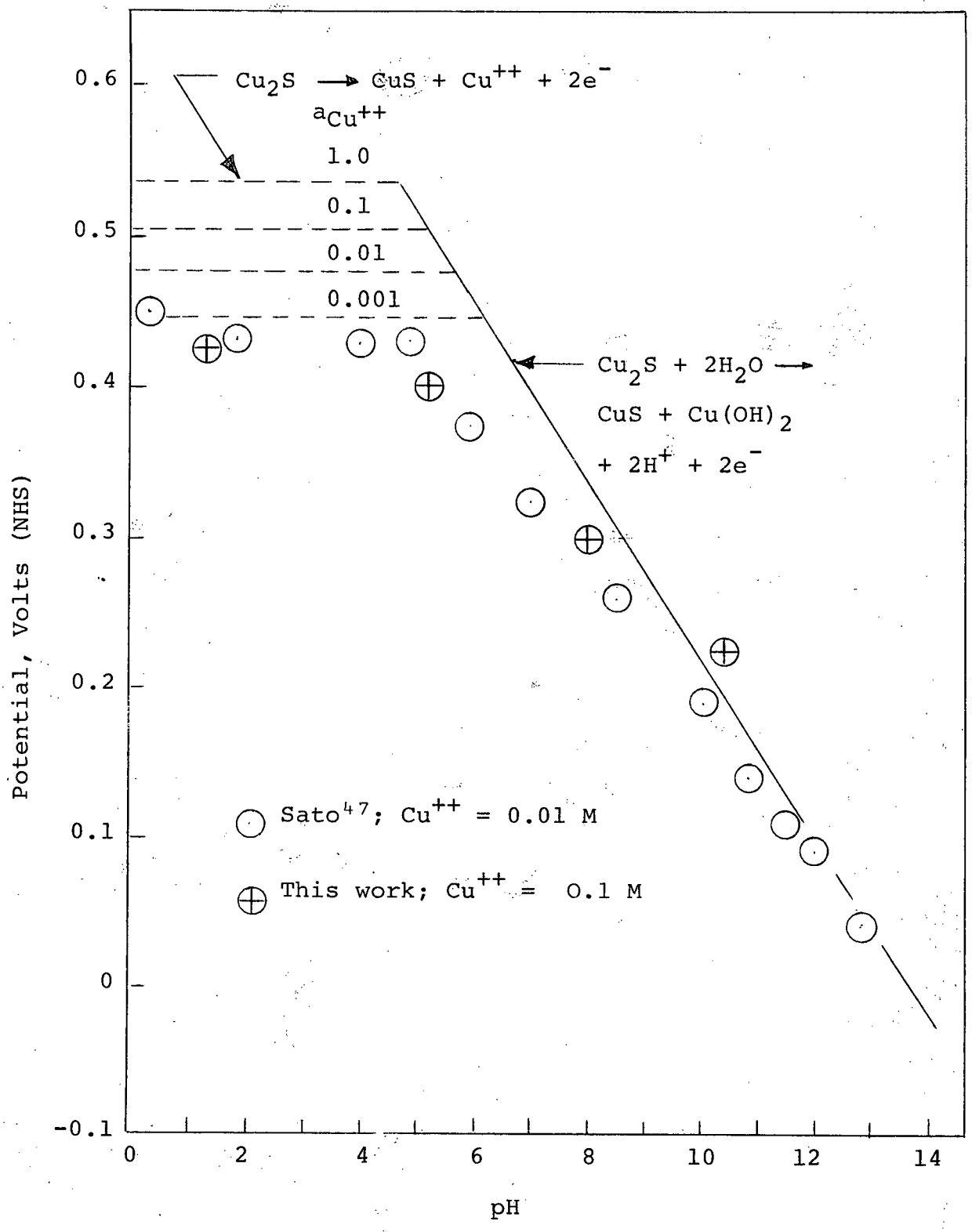


Figure 8. Potential of the $Cu_2S$ Electrode as a Function of pH

Preliminary Polarization Tests

The general shape of the anodic polarization curves is shown in Figure 9. There are three regions of note:

1. The region up to $\omega$ = 50 mV. In this region, the current density was very stable at a particular setting over periods of up to 10 hours. The points were also quite reproducible from test to test. Microscopic examination of the anode surface after 10 hours at $\omega$ = 25 mV showed little or no preferential grain boundary attack. When the current flow was stopped, the overpotential returned to approximately zero within a few seconds.

2. The region where $50 < \omega < 200$ mV. In this region, the polarization curves became less reproducible and there was considerable fluctuation with time of both the anode potential and the current density for a given cell potential. Microscopic examination of the anode surface after 60 hours at an overvoltage of approximately 150 mV showed considerable grain boundary attack (see Figure 10). When the current flow was stopped in this range, the overpotential returned to approximately zero within a minute. The fluctuations in this region are probably the result of rapid changes in the effective surface area of the anode due to preferential reaction at the grain boundaries.

3. The region beyond $\omega$ = 200 mV. The behaviour in this region was very erratic. The overpotential fluctuated over a range of about 50 mV even though the apparent current density was increasing. Microscopic examination of the anode after about 5 hours at an overpotential of about 250 mV showed more severe grain boundary attack than at lower overpotentials. The open circuit decay of the overpotential took a considerable length of

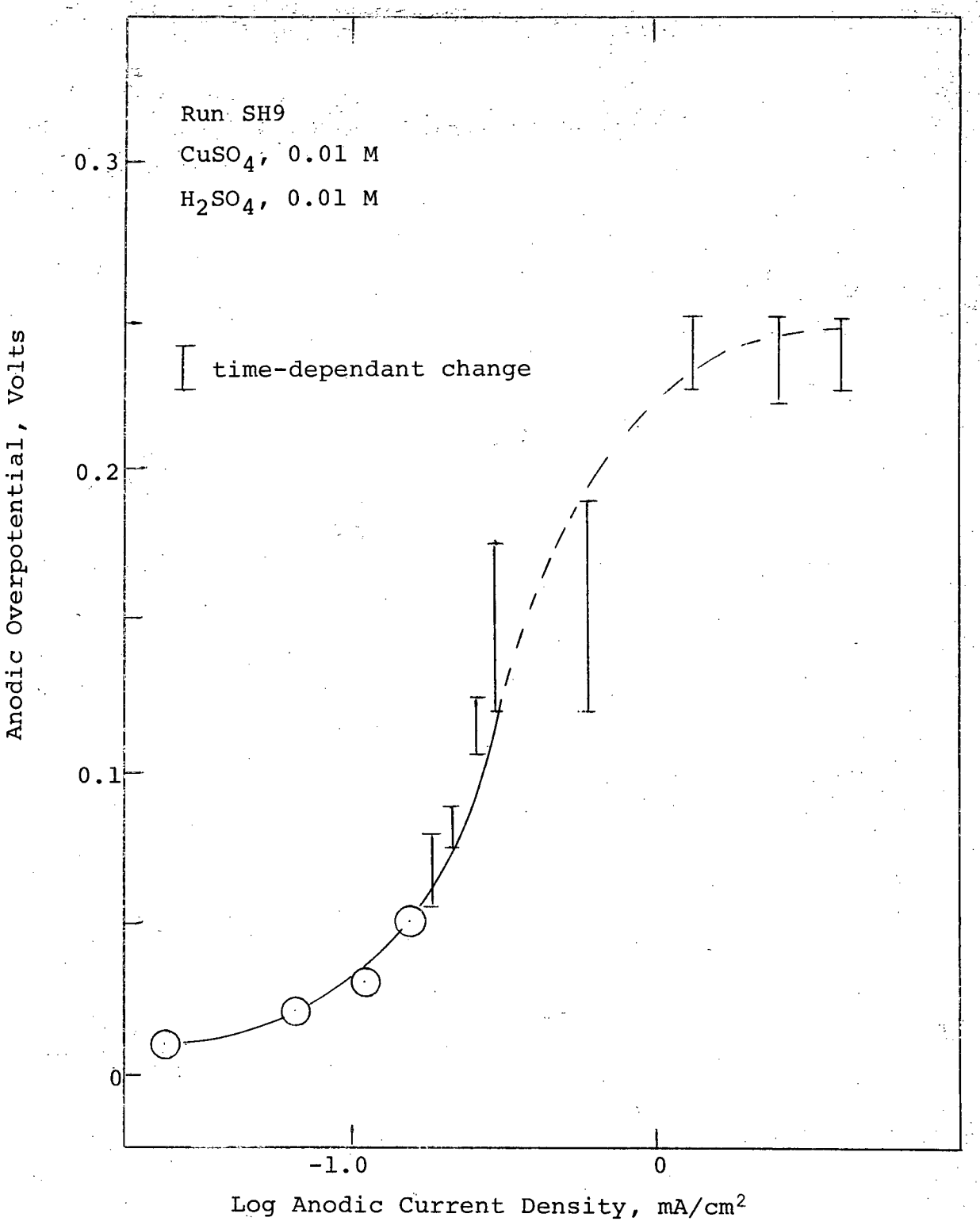


Figure 9. Typical Polarization Curve for Cuprous Sulphide Anode at 25° C

(a)

(b)

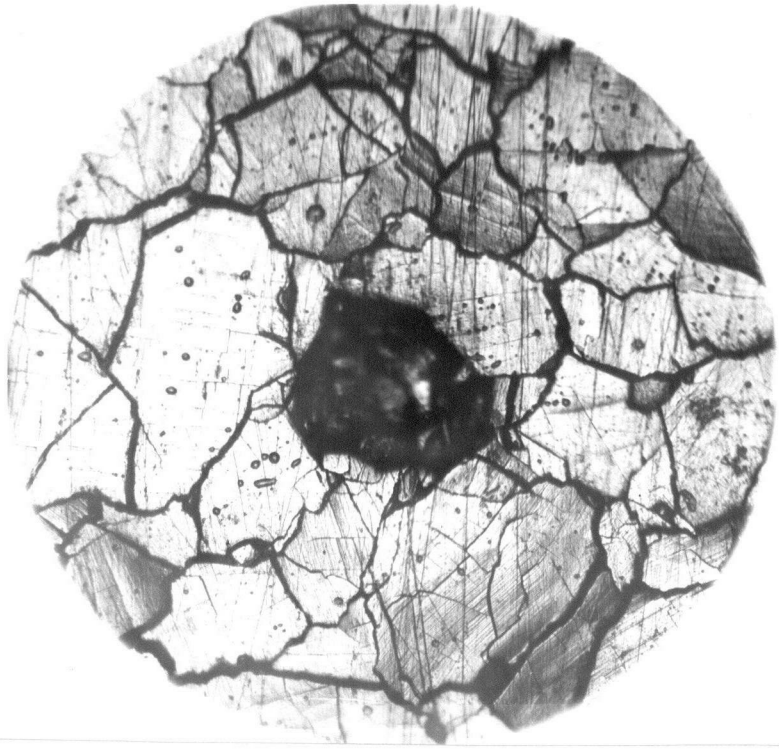

Figure 10. Cuprous Sulphide Anode Surface (a) before and (b) after Polarization at $\omega$ = 0.15 volts for 60 hours in 0.01 M $CuSO_4$, 0.1 M $H_2SO_4$ at 25-30° C

time and an example is illustrated in Figure 11. Such behaviour would be consistent with the existence of a difficultly soluble film on the anode surface, but there was no visible indication of such a film in these runs.

Stern[20,21] has shown that the difference in the slope of the polarization line in regions 1 and 2 is not necessarily the result of the presence of a second electrode reaction, but in this case, region 2 might well be a transition region between two electrode reactions i.e.

$$Cu_2S \longrightarrow CuS + Cu^{++} + 2e^- \quad .....(30)$$

$$CuS \longrightarrow Cu^{++} + S + 2e \quad .....(31)$$

The electrode potentials of the two reactions are quite similar (0.535 and 0.588 V respectively). It is possible that one reaction is occurring on the grain surfaces while the other is occurring at the grain boundaries.

Kinetic Parameters in Low Overpotential Region

The region up to $\omega$ = 0.05 V was studied further to provide data to test the kinetic relationships outlined in the Introduction. Typical polarization curves obtained in 0.1 M $H_2SO_4$ - 0.1 M $CuSO_4$ solutions are plotted in Figures 12 and 13 (semilogarithmic and arithmetic plots respectively). Values of $i_0$ (the exchange current), $\lambda$ (the stoichiometric factor) and $\beta$ (the symmetry factor) have been calculated from the slopes of these lines and are tabulated in Table XII. The straight portions of the logarithmic plots are quite short, so considerable inaccuracy is probably introduced to values of $d\omega/d \log i_A$, and then to $i_0$, $\lambda$ and $\beta$. In fact,

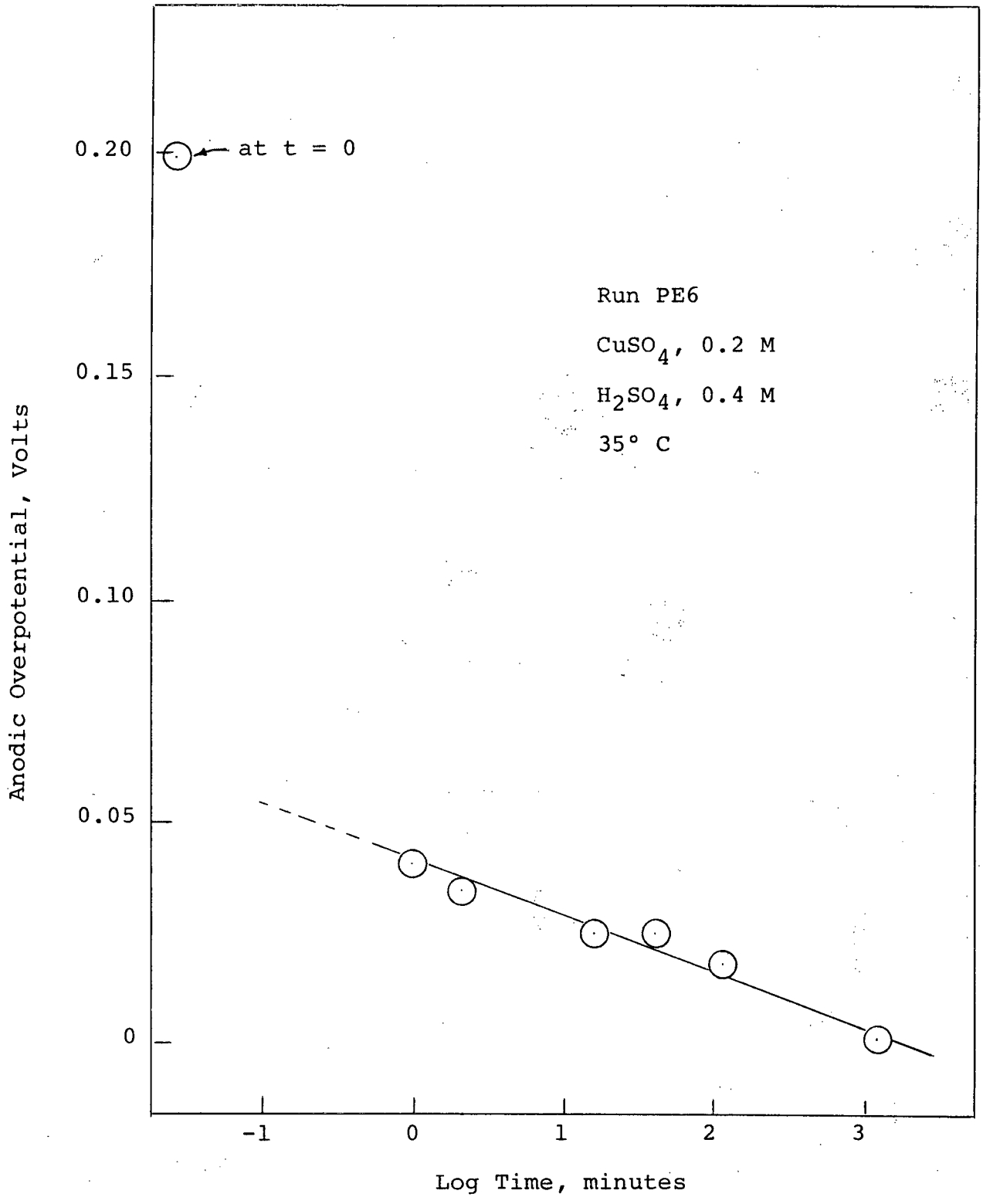


Figure 11. Decay of Anodic Overpotential with Time

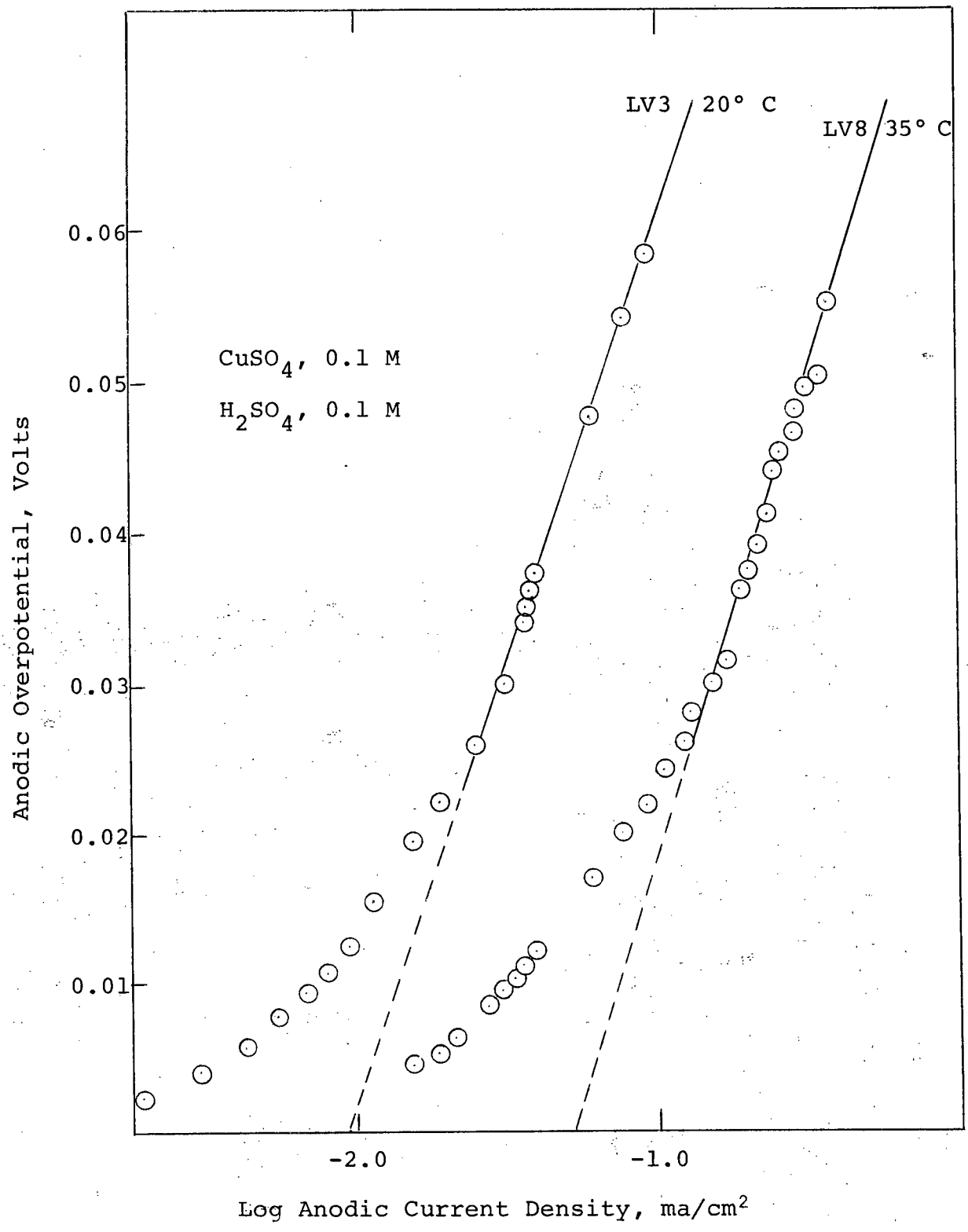


Figure 12. Example Curves: Effect of Temperature on the Polarization of $Cu_2S$ Anode

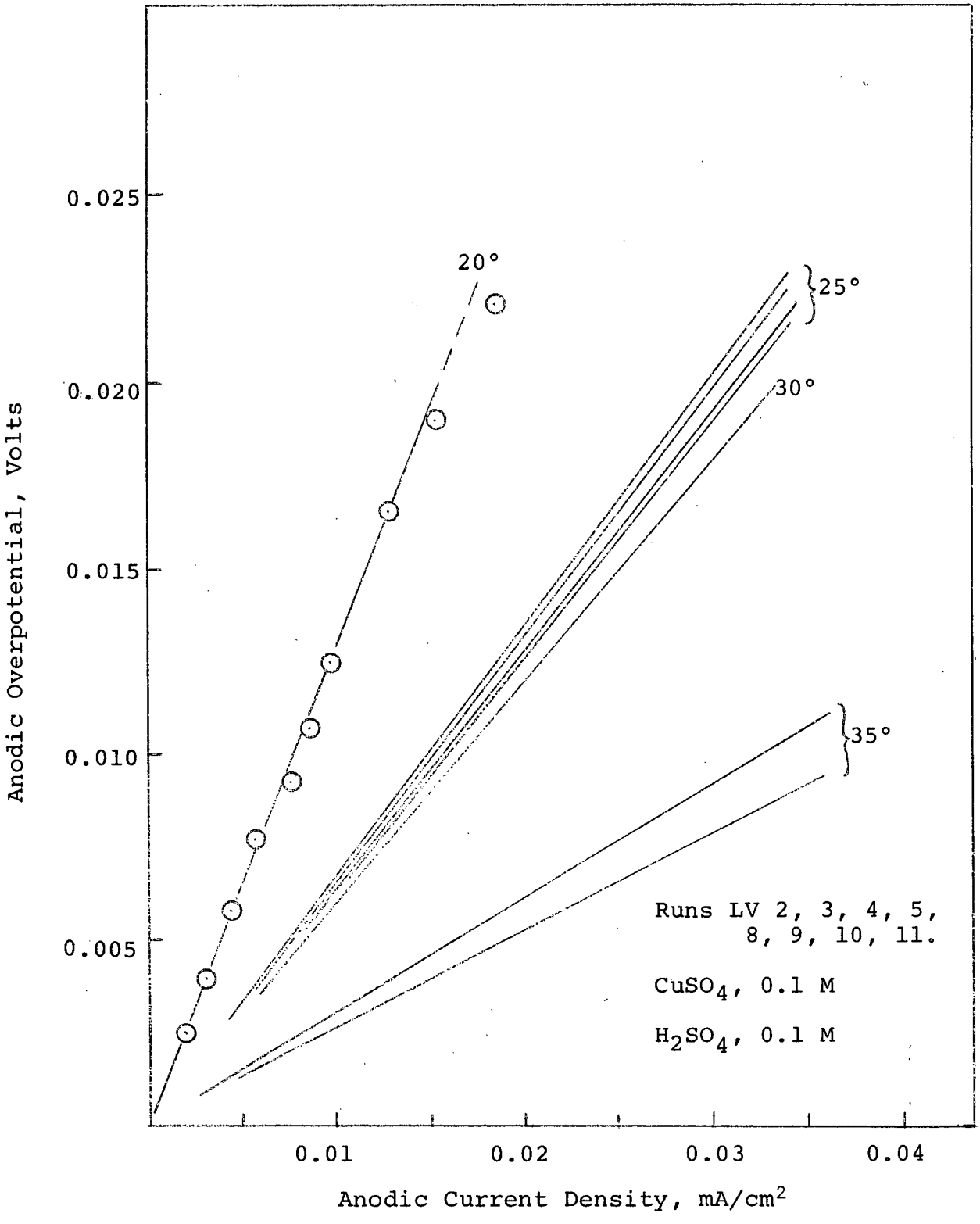


Figure 13. Effect of Temperature on Polarization of $Cu_2S$ Anode at Low Overpotentials (Experimental points omitted with one exception to simplify plot.)

TABLE XII

$i_0$, $\lambda$ and $\beta$ for the Cuprous Sulphide Anode

| Run No. | Temperature °C | $d\omega/di_A$ V/A/cm$^2$ | $d\omega/d \log i_A$ V | $i_0 \times 10^5$ S/cm$^2$ | $\lambda$ | $\beta$ |
|---|---|---|---|---|---|---|
| LV 3 | 20 | 1360.0 | 0.0588 | 0.95 | 1.96 | 0.5 |
| LV 2 | 25 | 642.5 | 0.0591 | 1.95 | 2.05 | 0.51 |
| LV 10 | 25 | 662.5 | 0.0616 | 2.14 | 1.81 | 0.47 |
| LV 11 | 25 | 677.5 | 0.0623 | 2.16 | 1.76 | 0.46 |
| LV 9 | 25 | 640.0 | 0.0612 | 2.12 | 1.89 | 0.49 |
| LV 4 | 30 | 597.5 | 0.0668 | 2.62 | 1.67 | 0.45 |
| LV 5 | 35 | 262.5 | 0.0647 | 4.95 | 2.04 | 0.54 |
| LV 8 | 35 | 305.0 | 0.0645 | 5.3 | 1.64 | 0.42 |

Stern[20,21] states that the straight line portion should extend over several logarithmic units to provide parameters of good accuracy. Both $\lambda$ and $\beta$ generally have values involving integers (e.g. $\lambda$ = 1, 2, 3; $\beta$ = 1/4, 1/3, 1/2) and the values from Table XII are close to $\lambda = 2$ and $\beta = 1/2$, so these values will be used in the following calculations.

It was stated earlier that

$$\omega = \frac{RT}{\mathcal{F}} \frac{i_A}{i_0 \lambda} \qquad \ldots\ldots(32)$$

This can be rewritten:

$$\left[\frac{d\omega}{di_A}\right]_{\omega \to 0} = \frac{RT}{\mathcal{F}} \frac{1}{i_0 \lambda} \qquad \ldots\ldots(33)$$

Values of $\frac{d\omega}{di_A}$ were quite precise (Figure 13) so using $\lambda = 2$, corrected values of $i_0$ were calculated (Table XIII). Further, using the corrected values of $i_0$, and $\lambda = 2$ and $\beta = 1/2$, corrected values of $d\omega/d \log i_A$ were calculated (Table XIII) which fit the experimental points quite well (Figure 14).

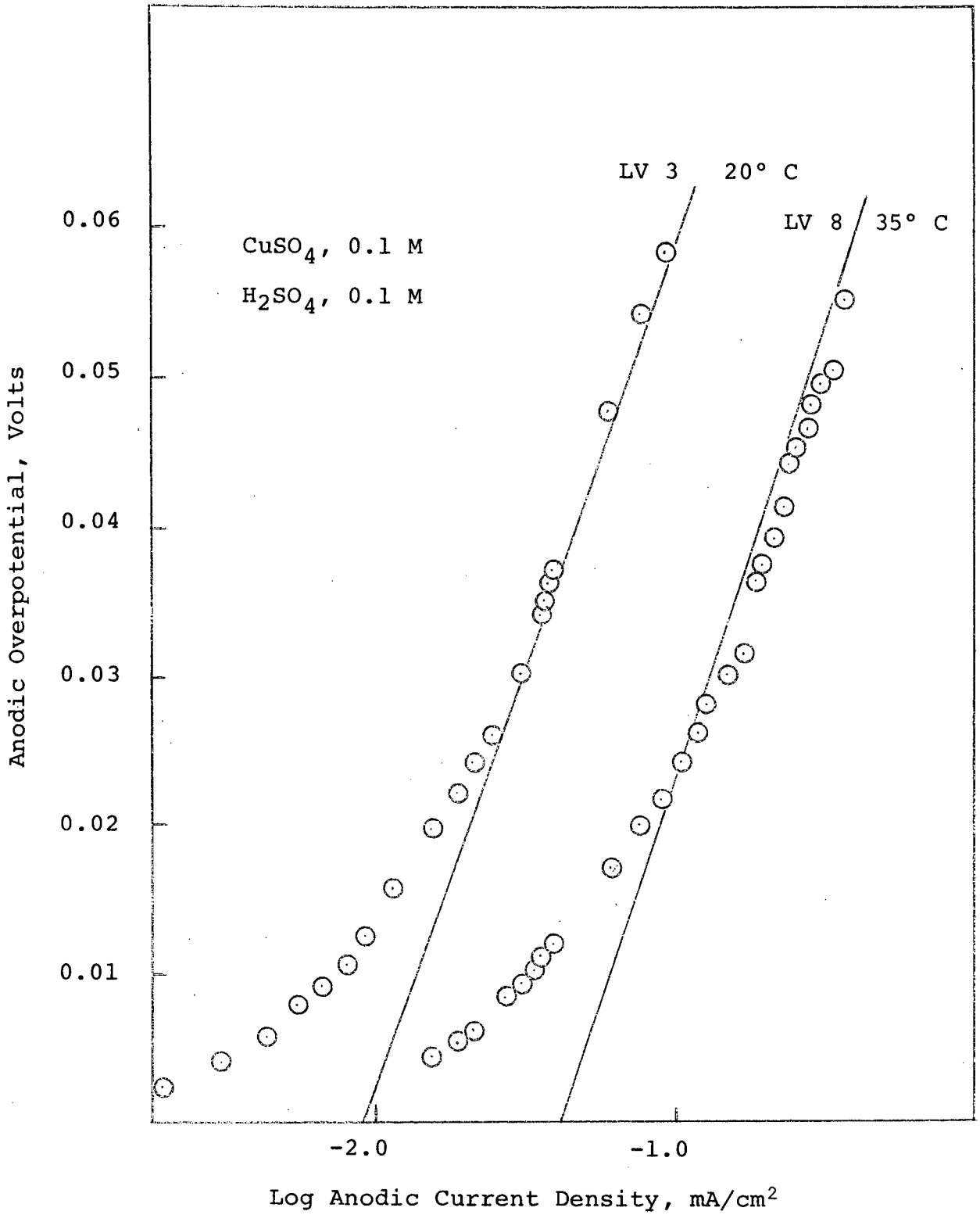


Figure 14. Fit of Recalculated Line to Experimental Data

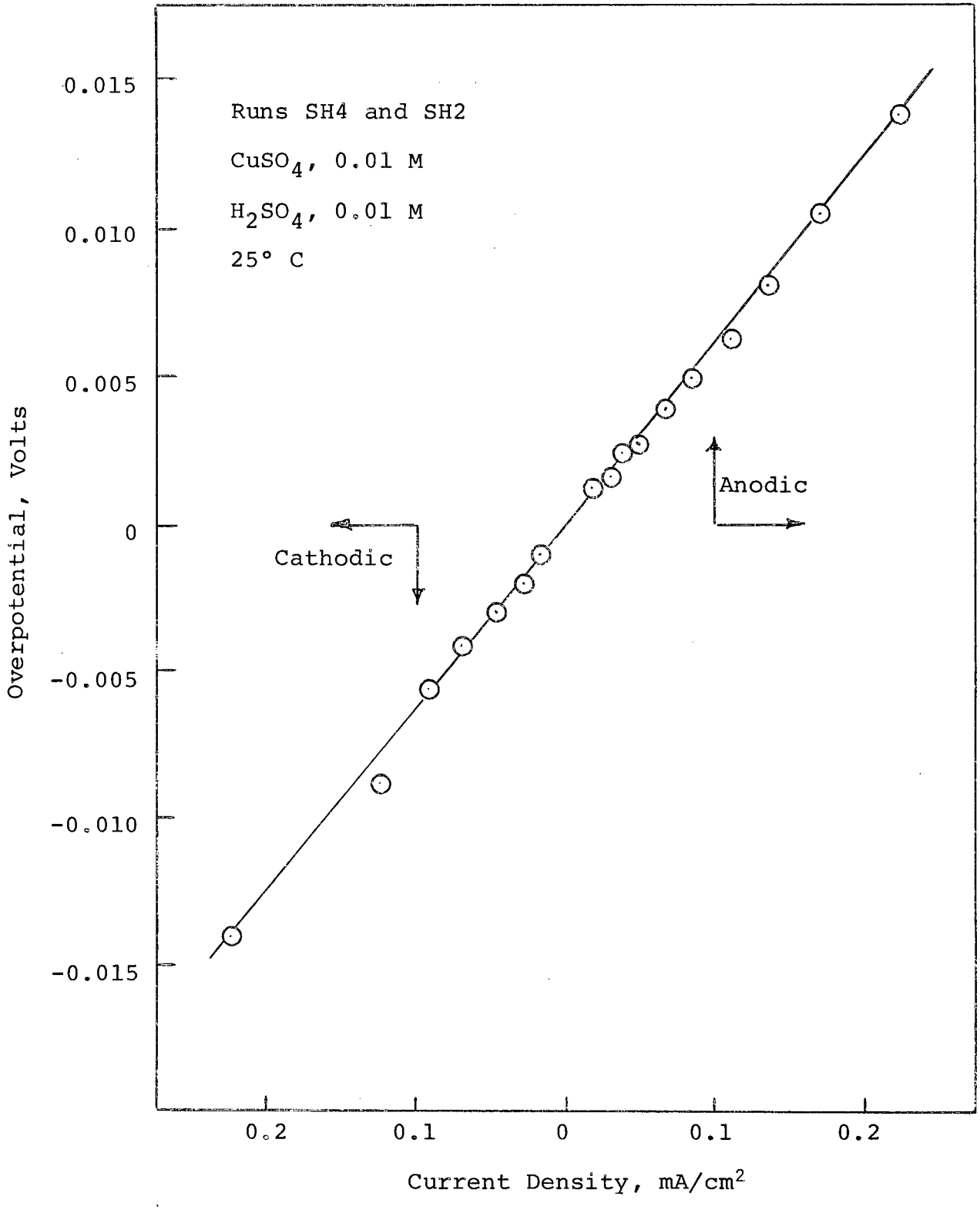


Figure 15. Anodic and Cathodic Polarization Curves for the $Cu_2S$ Electrode at Low Overpotentials

Examples of the anodic and cathodic polarization curves for the cuprous sulphide electrode (Figure 15) show little or no discontinuity. This lack of discontinuity at and near $\omega = 0$ has been interpreted by Stern and Geary[20] to indicate that only one oxidation-reduction reaction system is operating at the electrode.

TABLE XIII

Corrected Values of $i_0$ and $d\omega/d \log i_A$

| Run No. | Temperature °C | $i_0 \times 10^5$ A/cm$^2$ | $d\omega/d \log i_A$ V |
|---|---|---|---|
| LV 3 | 20 | 0.93 | 0.0582 |
| LV 2 | 25 | 2.00 | 0.0591 |
| LV 10 | 25 | 1.94 | 0.0591 |
| LV 11 | 25 | 1.90 | 0.0591 |
| LV 9 | 25 | 2.01 | 0.0591 |
| LV 4 | 30 | 2.19 | 0.0601 |
| LV 5 | 35 | 5.06 | 0.0611 |
| LV 8 | 35 | 4.35 | 0.0611 |

Reaction Products

A cuprous sulphide anode was oxidized in a 0.1 N perchloric acid solution at about 30°C with a current flow of about ten mA/cm$^2$ and $\omega = 0.2$ V. After 18 days, the anode was severely corroded. The remaining material was washed thoroughly in carbon bisulphide to remove any free sulphur and the residue was washed in alcohol and dried under vacuum. The residue was analysed for Cu and S, with the following results:

Cu = 63.9 wgt. %

S = 35.2 wgt. %

Cu/S atomic ratio = 0.916

The residue is therefore probably CuS. An x-ray powder picture was taken of a portion of the residue, and the resulting pattern is very similar to one obtained from chemically pure CuS (Appendix H). The electrolyte was analysed at the completion of the test for dissolved compounds of S (valence states lower than +6); there was no indication of the presence of S. No attempt was made to analyse for free sulphur in the corrosion residue.

Effect of Temperature on Polarization Curves

The reaction rate increases with temperature in the range 20°C to 35°C (Figure 13). Although the range of temperatures studied was quite small, a similar relationship probably exists over a much wider range.

Calculation of $\Delta H_o^*$

A value of $\beta = 1/2$ has been accepted after analysis of the polarization data. With this condition[N], a value of $\Delta H_o^*$, the heat of activation, can be calculated by the method of Hurlen[34] (Appendix F). The main relationship is restated below:

$$\Delta H_o^* = 2.303\ R\ \frac{d\ \log(J_o/T)}{d\ (1/T)} + \frac{1}{2}\Delta H_o \qquad \ldots\ldots(34)$$

Values of log $(J_o/T)$ were calculated (Table XIV) and plotted against the reciprocal temperature (Figure 16), and the best fit line gave

$$-2.303\ R\ \frac{d\ \log\ (J_o/T)}{d\ (1/T)} = 14.9\ \text{kcal/mole} \qquad \ldots\ldots(35)$$

---

N In addition to $\beta = 1/2$, K (the transmission coefficient) and $\nu$ (the frequency factor) should be the same for both the forward and reverse reaction across the activation barrier. It is generally assumed that these conditions hold true.

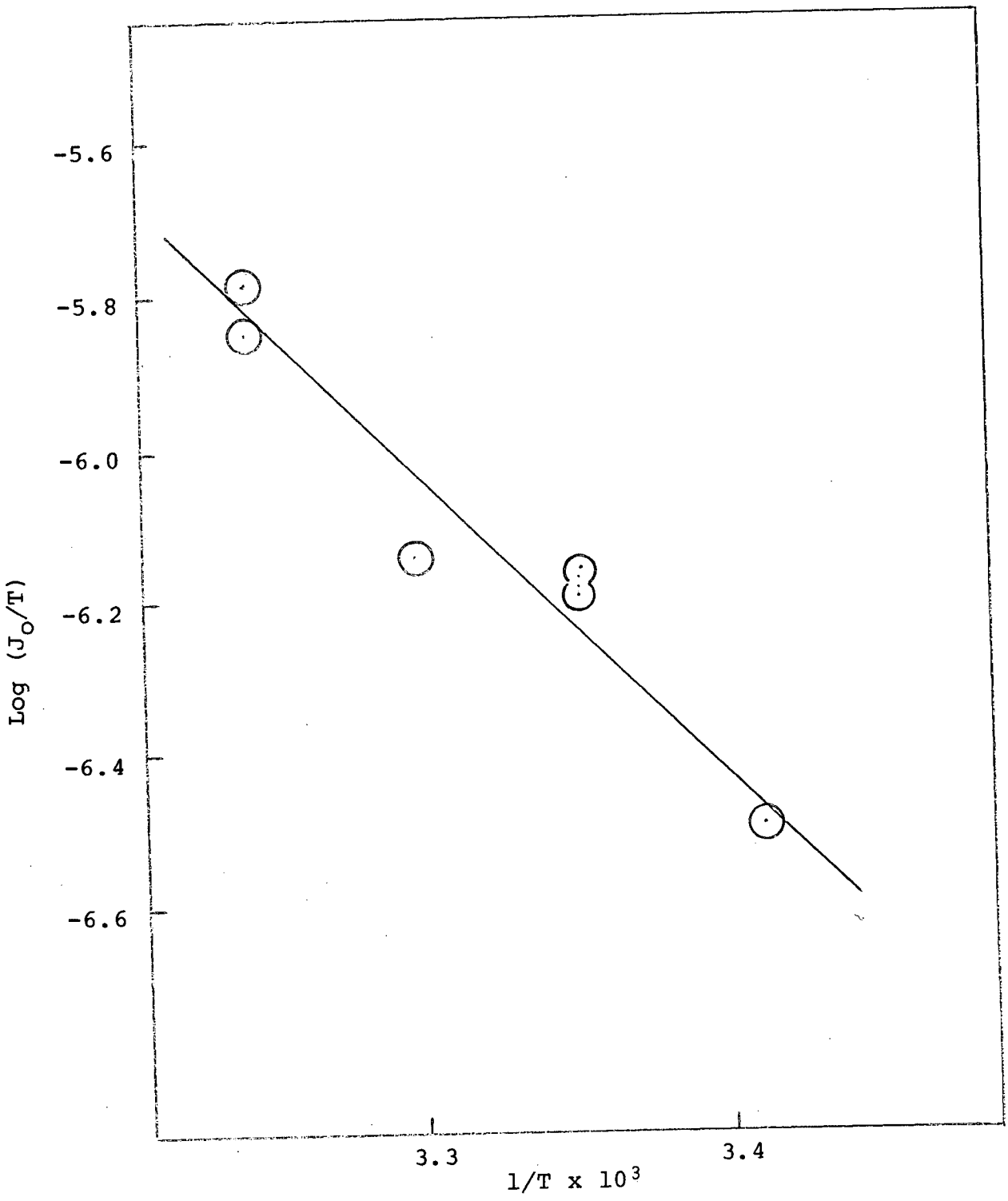


Figure 16. Plot of log ($J_o$/T) vrs (1/T): Determination of $\Delta H_o$* for the Cuprous Sulphide Electrode

TABLE XIV

Calculation of log ($J_o/T$)

| Run No. | $i_0 \times 10^5$ | $J_o \times 10^5$ | Temperature °K | $1/T \times 10^3$ | $\frac{J_o}{T} \times 10^7$ | log $J_o/T$ |
|---|---|---|---|---|---|---|
| LV 3 | 0.93 | 9.3 | 293 | 3.411 | 3.17 | -6.498 |
| LV 2 | 2.00 | 20.0 | 298 | 3.354 | 6.71 | -6.174 |
| LV 10 | 1.94 | 19.4 | 298 | 3.354 | 6.51 | -6.187 |
| LV 11 | 1.90 | 19.0 | 298 | 3.354 | 6.37 | -6.196 |
| LV 9 | 2.01 | 20.1 | 298 | 3.354 | 6.74 | -6.172 |
| LV 4 | 2.19 | 21.9 | 303 | 3.299 | 7.22 | -6.141 |
| LV 5 | 5.06 | 50.6 | 308 | 3.245 | 16.4 | -5.785 |
| LV 8 | 4.35 | 43.5 | 308 | 3.245 | 14.11 | -5.850 |

If the overall reaction is

$$Cu_2S \longrightarrow CuS + Cu^{++} + 2e^-, \qquad .....(36)$$

then when the value of $\Delta H°$ for this reaction (23.3 kcal/mole) is placed in equation (35), a value of 26.5 kcal/mole is obtained for $\Delta H_o^*$. This value can be compared with 15.2 kcal/mole determined by Hurlen for the $Cu/Cu^{++}aq$ electrode.

$\Delta H_o^*$ is a mean value between the values of $\Delta H_o^*$ (cathodic) and $\Delta H_o^*$ (anodic), these latter values being relative to the hydrogen scale. The accuracy of the value of $\Delta H_o^*$ calculated herein is about $\pm$ 7 kcal/mole. Because of this inaccuracy and the difficulty of relating the hydrogen scale values and absolute scale values, no further interpretation of this information has been attempted.

The Reaction Mechanism

The experimental results are consistent with the following low overpotential anodic oxidation reaction for cuprous sulphide:

$$Cu_2S \longrightarrow CuS + Cu^{++} + 2e \quad .....(37)$$

The evidence of CuS as a reaction product appears to be reasonable, but it was not demonstrated that free sulphur was absent as a reaction product. Therefore, it is possible that a second reaction was also occurring, viz:

$$CuS \longrightarrow Cu^{++} + S + 2e \quad .....(38)$$

The previously discussed work of Warren[49], Sullivan[50] and Sato[47] would indicate that the two reactions should occur during the complete oxidation of $Cu_2S$, but whether they were occurring simultaneously or consecutively in the present case is not known. The observation of severe grain boundary corrosion at overpotentials above about 50 mV would be consistent with the development of a surface film of poorly conducting, non-porous CuS on the grain surfaces, but such films were not observed.

If the low overpotential polarization reaction involved only (37), then the calculated kinetic parameters are consistent with the following reaction steps:

$$2\ Cu^{+}{}_{Cu_xS} \longrightarrow 2\ Cu^{+\oplus}{}_{Cu_xS} + 2e^{-} \quad .....(a) \qquad (39)$$

$$Cu^{+\oplus}{}_{Cu_xS} \longrightarrow Cu^{++}aq \quad .....(b)$$

In this case, two copper ions in the solid are involved when one copper ion is transferred into the solution. Possible rate controlling steps are:

(a) the creation of a cupric ion (i.e. electron hole) in the solid by the removal of an electron:

$$Cu^{+}{}_{Cu_xS} \longrightarrow Cu^{+\oplus}{}_{Cu_xS} + \ominus_{Cu_xS} \quad .....(40a)$$

(b) the removal of an electron through the external circuit:

$$\ominus_{Cu_xS} \longrightarrow e^- \text{(in external circuit)} \qquad \text{.....(40b)}$$

(c) transfer of electron between two sites in the solid:

$$\left|\ominus_{Cu_xS}\right|\text{Site 1} + \left|Cu^{+\oplus}{}_{Cu_xS}\right|\text{Site 2}$$

$$\longrightarrow \left|Cu^{+}{}_{Cu_xS}\right|\text{Site 2} \qquad \text{.....(40c)}$$

(d) dissolution of cupric ion:

$$Cu^{+\oplus}{}_{Cu_xS} \longrightarrow Cu^{++}aq \qquad \text{.....(40d)}$$

Reactions (40a) and (40c) are probably quite rapid because of the fairly large electronic conductivity in $Cu_2S$ (see Table II). Additional experimental work would be required to differentiate between steps (40b) and (40d). The simplest method would be to determine the influence, if any, of ($Cu^{++}aq$) on the reaction rate.

Although the value of $\Delta H_o^*$ is of questionable accuracy, it is in the range usually found for activation-controlled electrochemical reactions. A much larger value (say > 50 kcal/mole) would be expected if the rate was controlled by mass transfer through a film, unless of course the film is very porous.

# CONCLUSIONS

1. Rest potential measurements on an artificial cuprous sulphide electrode in acidified copper sulphate solution gave $V° = 0.490$ volts for the electrode potential.

2. In solutions of pH<4, the relationship between the electrode potential and $(Cu^{++})$ was consistent with the Nernst equation.

3. For the reaction:

$$Cu_2S \rightarrow CuS + Cu^{++} + 2e^-,$$

the calculated half cell potential $V°$ is $0.535 \pm 0.13$ volts. Although the experimental value of 0.490 volts is within the limits of accuracy of the calculated value, the experimental electrodes had a large Cu deficiency which may account for at least a portion of the discrepancy.

4. In solutions of pH>4, the rest potential measurements were consistent with the following electrode reaction:

$$Cu_2S + 2H_2O \rightarrow CuS + Cu(OH)_2 + 2H^+ + 2e^-$$

5. Polarization measurements at low overpotential gave values for the following kinetic parameters:

$\beta$, the symmetry factor = 1/2

$\lambda$, the number of electrons involved in each act of the rate determining step = 2

$i_o$, the exchange current $\approx 2 \times 10^{-5}$ A/cm$^2$

$\Delta H_o^*$, the standard heat of activation = 26.5 kcal/mole

6. CuS was tentatively identified as a reaction product, but the presence or absence of S was not determined. Therefore, it is not known to what extent the reaction:

$$CuS \longrightarrow Cu^{++} + S + 2e^{-}$$

took part in the overall oxidation.

7. The apparent absence of a surface film and the value of $\Delta H_o^*$ indicate that the anodic oxidation reaction is activation controlled, rather than bulk mass transfer controlled, at least at low values of the overpotential.

## RECOMMENDATIONS FOR FUTURE INVESTIGATIONS

1. The effect of ($Cu^{++}$) on the reaction rate should be determined to clarify the reaction mechanism.

2. A series of $Cu_xS$ electrodes should be prepared with different Cu/S ratios in order to assess the influence of stoichiometry on the electrode potential. Solid-state electrolytic cells[7-10] could be used to prepare the electrodes. Single crystal surfaces would probably be desirable.

3. Investigations at higher overpotentials would be of considerable interest, but a more sophisticated measuring circuit should be used. For example, polarization techniques wherein a square wave alternating current is used can provide information on the nature of passivating films.

4. Polarization studies should be extended to higher temperatures and to include more corrosive solutions.

REFERENCES


1. L. S. Renzoni, R. C. McQuire and M. V. Barker, AIME preprint, New York, (1958).

2. L. S. Renzoni, R. C. McQuire and M. V. Barker, J. Metals, 10, 414 (1958).

3. K. Sproule, G. A. Harcourt and L. S. Renzoni, ibid., 12, 214 (1960).

4. T. S. Licht and A. J. deBethune, J. Chem. Ed., 34, 433 (1957).

5. J. S. Anderson and M. C. Morton, Proc. Royal Soc., A,184, 83 (1945).

6. W. C. Dunlap, "An Introduction to Semiconductors," John Wiley and Sons, New York 1957.

7. C. Wagner, J. Chem. Phys., 21, 1819 (1953).

8. J. Bruce Wagner and C. Wagner, ibid., 26, 1597 (1957).

9. J. Bruce Wagner and C. Wagner, ibid., 26, 1602 (1957).

10. H. Kobayashi and C. Wagner, ibid., 26, 1609 (1957).

11. W. Noddack and K. E. Wrabetz, Z. Elektrochem., 59, 96 (1955).

12. K. E. Wrabetz, ibid., 60, 722 (1956).

13. G. Kortum and J. O'M. Bockris, "Textbook of Electrochemistry," Elsevier, Amsterdam 1951.

14. J. O'M. Bockris, "Modern Aspects of Electrochemistry," (editor: J. O'M. Bockris), Butterworth Scientific Publications, London, volume 1 (1954), ch. 4.

15. Mino Green, ibid., volume 2 (1959) ch. 5.

16. R. A. Robinson and R. S. Jones, J. Am. Chem. Soc., 58, 959 (1936).

17. S. Glasstone, "Elements of Physical Chemistry," D. Van Nostrand Co. Inc., New York 1952.

18. G. N. Lewis and Merle Randall, "Thermodynamics," 2nd ed. (edited by: Pitzer and Brewer), McGraw Hill, New York 1961.

19. W. Latimer, "The Oxidation States of the Elements and Their Potential in Aqueous Solution," 2nd ed., Prentice Hall, Inc., Englewood Cliffs, N.J. 1952.

20. M. Stern and A. L. Geary, J. Electrochem. Soc., 104, 56 (1957).

21. M.Stern, ibid., 104, 559 (1957).

22. M.Stern, ibid., 104, 645 (1957).

23. R. Piontelli, G. Bianchi, U. Bertocci, C. Guerci and B. Rivolta, Z. Elektrochem., 58, 54 (1954).

24. Handbook of Chemistry and Physics, 35 ed., 1953-1954.

25. W. J. Argersinger, J. Phys. Chem., 58, 792 (1954).

26. V. F. Holland and O. D. Bonner, J. Am. Chem. Soc., 77, 5833 (1955).

27. M. Pourbaix, "Thermodynamics of Dilute Aqueous Solutions," Arnold, London 1949.

28. G. Valensi, CITCE, Compt. Rend. Reunion, 51 (1950).

29. R. Parsons, see reference 14, ch. 3.

30. Butler, "Electrocapillarity," Methuen, London 1940.

31. D. D. Eley and M. G. Evans, Trans. Faraday Soc., 34, 1093 (1938).

32. T. Hurlen, Acta Chem. Scan., 15, 630 (1961).

33. T. Hurlen, ibid., 14, 1533 (1960).

34. T. Hurlen, ibid., 14, 1564 (1960).

35. T. Hurlen, ibid., 15, 621 (1961).

36. F. D. Rossini, "Selected Values of Chemical Thermodynamic Values," U.S. Government Printing Office, Washington 1952.

37. J. Halpern, unpublished manuscript.

38. A. J. deBethune, J. Electrochem. Soc., 102, 288C (1955).

39. T. Hurlen, Acta Chem. Scan., 15, 630 (1961).

40. G. N. Lewis and Merle Randall, J. Am. Chem. Soc., 43, 1112 (1921).

41. L. Young, "Anodic Oxide Films," Academic Press, New York 1961.

42. W. Ruhl and E. Saur, Ber. Ober. Ges. Naturund Heilkunde, 26-29, 35 (1954-1958).

43. M. Pourbaix and G. Govaerts, "First International Congress on Metallic Corrosion," 1961, Butterworth, London 1962.

44. M. Hansen, "Constitution of Binary Alloys," McGraw Hill, New York 1958.

45. R. Schuhmann and O. W. Moles, J. Metals, 3, 235 (1951).

46. M. Sato, Econ. Geol., 55, 928 (1960).

47. M. Sato, ibid., 55, 1202 (1960).

48. J. Horvath and M. Novak, Cor. Sco., 4, 159 (1964).

49. I. H. Warren, Aus. J. App. Sci., 9, 36 (1958).

50. J. D. Sullivan, USBM Tech. paper 473 (1930).

51. J. F. Elliott and M. Gleiser, "Thermochemistry for Steelmaking," Addison-Wesley, Reading 1960.

52. T. Rosenqvist, J. Iron Steel Inst., 176, 37 (1954).

53. B. E. Conway, "Electrochemical Data," Elsevier, London 1952.

54. F. Fenwick, J. Am. Chem. Soc., 48, 860 (1926).

55. H. Britton, J. Chem. Soc., 127, 2110 (1925).

56. G. J. Janz and D. J. G. Ives, "Reference Electrodes," Academic Press 1961.

57. N. W. Buerger, Econ. Geol., 36, 19 (1941).

58. P. Rahlfs, Z. physik. Chem., B31, 184 (1936).

59. A. S. Powarennych, Geologie, 4, 377 (1963).

60. A. J. deBethune, T. S. Licht and N. Swendeman, J. Electrochem. Soc., 106, 616 (1959).

61. P. E. J. Aylen, Research Report, University of British Columbia, April 1959.

62. E. Hirahara, J. Phys. Soc. Japan, 6, 422 (1951).

63. E. Hirahara, ibid., 6, 428 (1951).

64. N. W. Lord and D. J. Demarest, "Metallurgical Analysis," McGraw Hill, New York 1924.

# APPENDIX A

## Anodic Oxidation of Tin Sulphide

Considerable time was expended initially on a study of electrochemical oxidation in the Sn-S system. Although this work was terminated because of the lack of reproducibility of the experimental data, the results and problems encountered are summarized here for consideration in future work.

### Preparation of Tin Sulphide

Stannous sulphide was prepared by carefully mixing stoichiometric amounts of molten Sn and S in an evacuated Vycor tube. After mixing appeared to be complete, the SnS was placed in a muffle furnace and held at 900°C to encourage homogeneity. By slow cooling of the furnace through the melting temperature of SnS (approximately 880°C), it was expected that the material would solidify as either a single crystal or a series of large crystals. However, it usually solidified as a small dense portion topped by a very porous network of dendrites. One of the better pieces was analysed and mounted in a manner similar to that used with the $Cu_2S$. The material analysed (one analysis) about 67% Sn (analytical method: iodine titration) compared to 78.8% Sn for stoichiometric SnS and 65% in stoichiometric $SnS_2$. The Sn deficiency is surprising: the tin sulphide could well be a mixture of SnS, $SnS_2$ and Sn, but the analysis of a reasonably large piece of material should reflect the original stoichiometry. The result, of course, is suspect as only one analysis was performed. The exact composition of the tin sulphide is thus unknown.

Potential Measurements

Some rest potential measurements in $SnCl_2$ solutions are summarized in Table A-I.

TABLE A-I

Rest Potentials for Tin Sulphide Electrode at 25°C in $SnCl_2$ Solution

| Run Number | $Sn^{++}$ M | $H^+$ M | pH | Anode Potential w.r.t. Calomel V |
|---|---|---|---|---|
| SE 1 | 0.091 | 0.568 | 0.35 | -0.074 |
| 2 | 0.084 | 0.592 | 0.38 | -0.079 |
| 3 | 0.082 | 0.597 | - | -0.114 |
| 5 | 0.074 | 0.575 | 0.55 | -0.072 |
| 6 | 0.072 | 0.578 | 0.31 | -0.066 |
| 7 | 0.0374 | 0.25 | 0.25 | -0.072 |
| 8 | 0.0201 | 0.157 | 0.3 | -0.074 |
| 9 | 0.00358 | 0.0815 | 0.61 | -0.082 |

The average value is about -0.08 volts. Using the relationship

$$\mathcal{E}\ \text{cell} = V_{S.C.E.} - V_{anode}$$

then $V_{anode} = 0.2415 - (-0.08) = 0.32$ V

where $V_{anode} = V°_{anode} + \frac{RT}{nf} \ln \frac{[\text{OX.}]}{[\text{RED.}]}$.

Several electrode reactions should be considered:

$$SnS \longrightarrow Sn^{++} + S + 2e^- \qquad V° = 0.253 \text{ V}$$

$$SnS_2 \longrightarrow Sn^{+4} + 2S + 4e^- \qquad V° = 0.418 \text{ V}$$

$$Sn^{++} \longrightarrow Sn^{+4} + 2e^- \qquad V° = 0.150 \text{ V}$$

The activity of $Sn^{++}$ is probably in the range 0.01-0.1 in the test solutions, so the measured anode potential corresponds to values of

$V°_{anode}$ in the range 0.35-0.38 V. The lack of agreement between the measured value and the theoretical values suggests that either some other reaction or a mixture of two or more of the above reactions was determining the electrode potential.

Polarization Curves

Nineteen preliminary kinetic runs were made, and the following general observations recorded:

1. The polarization curves were not unusual, as can be seen in the example in Figure A-1. The straight line portion (semi-log plot) was fairly uniform over about two logarithmic cycles, but there was no measure of reproducibility from one run to the next.
2. The method of anode surface preparation had an important effect on the polarization curves. For example, a higher overpotential was necessary to achieve a certain current flow when the anode was cleaned with toluene than when freshly polished or etched slightly with acid.
3. After a number of days using the same solution, a gelatinous precipitate was observed at the bottom of the electrolytic cell. This material was not analysed, but was likely a hydrolysis product. For example $Sn^{+4}$ hydrolyses very readily as $Sn(OH)_4$. The pH should exceed 1.9 before the hydrolysis of $Sn^{+2}$ becomes dominant[55]. No further comment can be made without the analysis of the material.

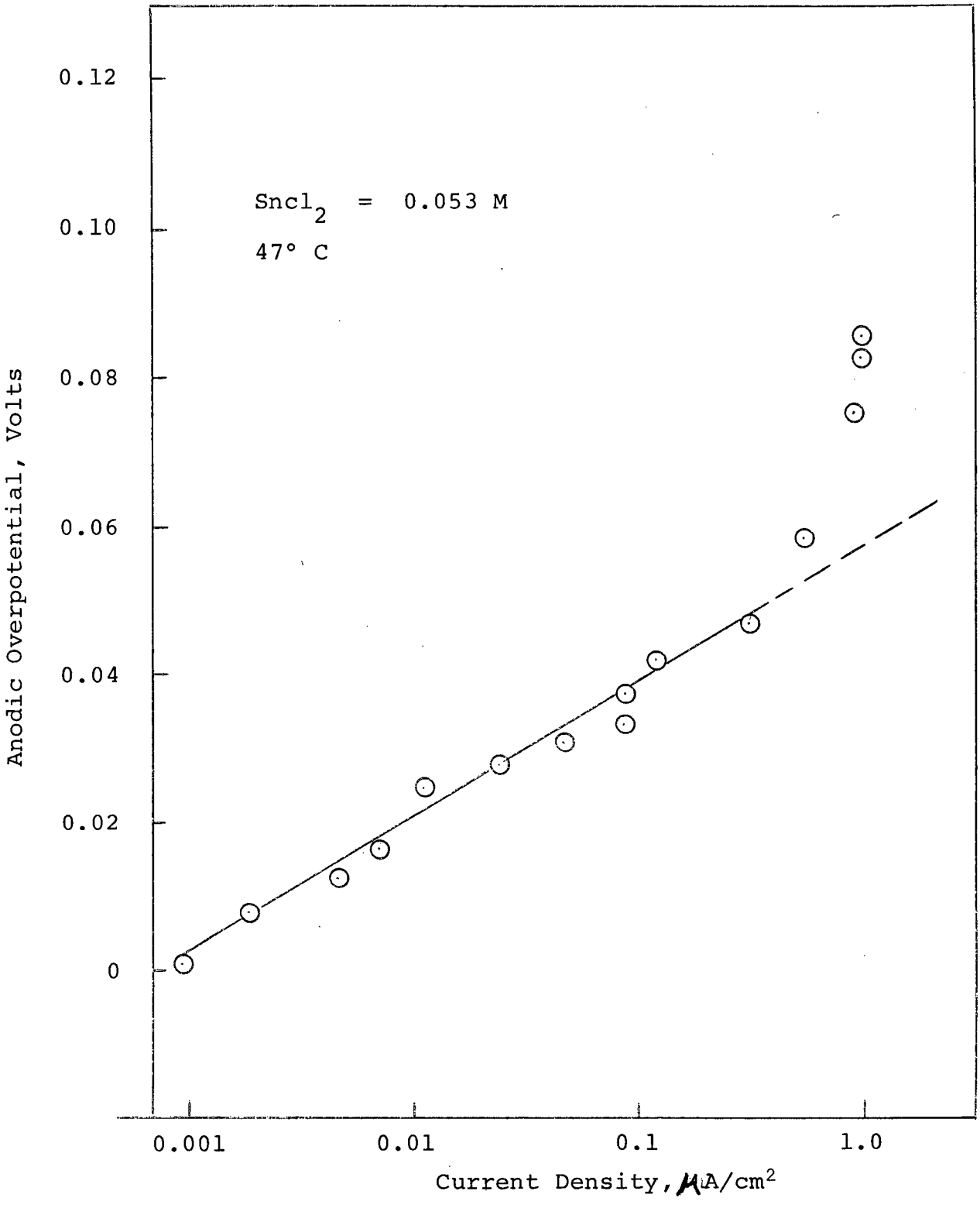


Figure A1. Anodic Polarization Curve for Tin Sulphide Electrode

4. Reproducible results were unobtainable with this particular tin sulphide electrode.

On the basis of these observations and because of the great difficulty experienced in the attempt to produce a satisfactory electrode, the work with tin sulphide was terminated.

# APPENDIX B

## Sign Convention for Electrochemical Measurements

An area of considerable confusion in electrochemical studies centres around the sign of electrode potentials and voltages in electrochemical cells. The convention used in this work is patterned after that proposed by deBethune[4] and is consistent with the IUPAC - Stockholm convention[55]. The essential feature is that each half cell in an electrochemical cell is assigned an electrode potential which is independent of the direction in which the half cell is written.

To start, the terms "anode" and "cathode" are defined. An anode is an electrode where oxidation is occurring or is assumed to occur by the chemical reaction written to describe that electrode, and a cathode is an electrode where reduction occurs or is assumed to occur, irrespective of whether the reaction is spontaneous or is forced by an external emf. Then for oxidation at an anode,

$$\Delta F_e = + n\mathcal{F}V_e$$

and for reduction at a cathode,

$$\Delta F_e = - n\mathcal{F}V_e$$

where $V_e$ is the electrode potential associated with a particular electrode reaction, regardless of whether oxidation or reduction is occurring at a particular moment. For example, if the oxidation of copper in a cupric solution is considered:

$$Cu \longrightarrow Cu^{++} + 2e^-$$

$$\Delta F^\circ = (\Delta F^\circ_{f(Cu^{++})} + 2\Delta F^\circ_{f(e^-)}) - (\Delta F^\circ_{f(Cu)})$$

$$= (15.5 + 0) - (0) = 15.5 \text{ kcal./mole}$$

$$\Delta F^\circ = + n\mathcal{F}V^\circ$$

$$V^\circ = + \frac{\Delta F^\circ}{n\mathcal{F}} = \frac{15.5}{2(23.06)} = 0.337 \text{ V}$$

Conversely, if the reduction of cupric ion at a copper cathode is considered:

$$Cu^{++} + 2e^- \longrightarrow Cu$$

$$\Delta F^\circ = \Delta F^\circ_{f(Cu)} - (\Delta F^\circ_{f(Cu^{++})} + 2\Delta F^\circ_{f(e^-)})$$

$$= 0 - (15.5 + 0) = 15.5 \text{ kcal./mole}$$

$$\Delta F^\circ = -n\mathcal{F}V^\circ$$

$$V^\circ = - \frac{\Delta F^\circ}{n\mathcal{F}} = - \frac{(-15.5)}{2(23.06)} = 0.337 \text{ V}$$

Thus an unambiguous potential* can be assigned to each electrode reaction, completely independent of the assumed direction of the electrode reaction.

To illustrate the use of the electrode potential in the thermodynamic treatment of whole cells, consider the iron-copper reaction in acid solution (i.e. the cementation reaction in copper refining). First consider the overall reaction:

$$Fe + Cu^{++} \rightleftharpoons Fe^{++} + Cu \qquad \text{.....(Reaction O)}$$

$$\Delta F_O = \Delta F_O^\circ + RT \ln \frac{a_{Fe^{++}}}{a_{Cu^{++}}}$$

$$\Delta F_O = -n\mathcal{F}\mathcal{E}_O \text{ and } \Delta F_O^\circ = -n\mathcal{F}\mathcal{E}_O^\circ$$

---

* The electrode potentials $V^\circ$ are numerically equal but opposite in sign to the oxidation potentials tabulated by Latimer[19].

Then $$\mathcal{E}_O = \mathcal{E}_O^\circ - \frac{RT}{n\mathcal{F}} \ln \frac{a_{Fe^{++}}}{a_{Cu^{++}}}$$

Now consider the half cells:

$$Fe \longrightarrow Fe^{++} + 2e \qquad V_F^\circ = 0.440 \text{ V} \quad \text{.....(Reaction F)}$$

$$\Delta F_F = \Delta F_F^\circ + RT \ln a_{Fe^{++}}$$

$$\Delta F_F = + n\mathcal{F} V_F \text{ and } \Delta F_F^\circ = + n\mathcal{F} V_F^\circ$$

$$Cu \longrightarrow Cu^{++} + 2e^- \qquad V_C^\circ = 0.337 \text{ V} \quad \text{.....(Reaction C)}$$

$$\Delta F_C = \Delta F_C^\circ + RT \ln a_{Cu^{++}}$$

$$\Delta F_C = + n\mathcal{F} V_C \text{ and } \Delta F_C^\circ = n\mathcal{F} V_F^\circ$$

But $$\Delta F_O = \Delta F_F - \Delta F_C$$

$$= \Delta F_F^\circ + RT \ln a_{Fe^{++}} - (\Delta F_C^\circ + RT \ln a_{Cu^{++}})$$

$$= n\mathcal{F}(V_F^\circ - V_C^\circ) + RT \ln \frac{a_{Fe^{++}}}{a_{Cu^{++}}}$$

But $$\Delta F_O = - n\mathcal{F} \mathcal{E}_O$$

Then $$\mathcal{E}_O = (V_C^\circ - V_F^\circ) - \frac{RT}{n\mathcal{F}} \ln \frac{a_{Fe^{++}}}{a_{Cu^{++}}}$$

$$\mathcal{E}_O^\circ = V_C^\circ - V_F^\circ$$

In the present case, the cell can be represented in the following way:

$$Fe, Fe^{++} \;||\; Cu^{++}, Cu$$

Then $$\mathcal{E}^\circ = V_C^\circ - V_F^\circ$$

$$= V^\circ(\text{right side}) - V^\circ(\text{left side})$$

Now $V_C^\circ = 0.337$ V, and $V_F^\circ = -0.440$ V

Then $$\mathcal{E}^\circ = 0.337 - (-0.440) = 0.777 \text{ V}$$

Now $$\Delta F^\circ = - n\mathcal{F} \mathcal{E}^\circ$$

so $$\Delta F^\circ = -2(23.06)(0.777) = 35.8 \text{ kcal/mole}$$

This is equal to the value, both numerically and in sign, calculated from the listed free energies. Therefore, it is concluded that the sign convention used here for the half cell potentials is consistent with standard thermodynamic conventions.

# APPENDIX C

## Compilation of Appropriate Thermodynamic Data

The thermodynamic data for the various chemical species of interest in this study are compiled in Table C-I. In most cases, they have been taken from standard sources - Elliott and Gleiser[51], Rossini[36] and Latimer[19]. The major exception is the free energy of the cuprous ion. It was calculated as shown below.

According to Fenwick[54], Keq = 1 x $10^6$ $\pm$10% at 25°C for the reaction

$$2\ Cu^{+} \rightleftharpoons Cu^{++} + Cu$$

Then $\Delta F° = -RT \ln Keq$

$= -8.18 \pm 0.8$ kcal/mole

Rossini[36] assigns $\Delta F_f°$ for $Cu^{++}$ equal to 15.5 kcal, Latimer[19] assigns 15.53 kcal and Lewis and Randall[18] assign 15.91 kcal. The chosen value was 15.5 $\pm$0.5 kcal. Then

$$\Delta F_f° \text{ for } Cu^{+} = 1/2 \left[ (\Delta F_f°)_{Cu^{++}} + (\Delta F_f°)_{Cu} - \Delta F° \right]$$

$$= 11.84 \pm 0.65 \text{ kcal/mole}$$

By using the relationship

$$\Delta H° = \Delta F° + T\ \Delta S°,$$

a value of 17.3 kcal/mole was calculated for $\Delta H_f°$ for $Cu^{+}$. Similarly,

$S°$ for $Cu(OH)_2$ = 16.1 e.u.

$S°$ for $Cu_2SO_4$ = 41.3 e.u.

The most recent values for the free energy and heat of formation of sulphides were given by Elliott and Gleiser[51] using $S_2$(gas) as the standard state. These have been converted for this

work using S (rhombohedral) as the standard state.

The possible errors or standard deviations were calculated in the following manner. Assume the relationship is

$$A + B = C$$

Take logarithms:

$$\ln (A+B) = \ln C$$

Differentiate:

$$d \ln (A+B) = d \ln C$$

Using the identity $\frac{dx}{x} = d \ln x$

convert to

$$\frac{d (A+B)}{(A+B)} = \frac{dC}{C}$$

$$\frac{dA + dB}{A + B} = \frac{dC}{C}$$

Replace differential with exact increment $\Delta$:

$$\frac{\Delta A + \Delta B}{A + B} = \frac{\Delta C}{C}$$

$\Delta A$, $\Delta B$ and $\Delta C$ are the standard deviations for A, B and C. If two of the values are known, the third can be calculated.

Using the data of Table C-I, the half cell potentials of a number of electrode reactions of interest in this work have been calculated, and are presented in Table C-II.

TABLE C-I: Thermodynamic Data at 298° K

| Species | Δ F°f kcal/mole | Δ H°f kcal/mole | S°, e.u. |
|---|---|---|---|
| $H^+$ | 0 (36) | 0 (36) | 0 (36) |
| $H_2(g)$ | 0 (36) | 0 (36) | 31.2 (36) |
| $e^-$ | 0 (36) | 0 (36) | 15.6 (36) |
| $O_2(g)$ | 0 (36) | 0 (36) | 49.0 (36) |
| $OH^-(aq)$ | -37.6 (36) | -55.0 (36) | -2.52 (36) |
| $H_2O$ | -56.69±0.02 (51) | -68.317±0.01 (51) | 16.7 (36) |
| Cu | 0 (51) | 0 (51) | 7.97 (51) |
| $Cu^+(aq)$ | 11.84±0.65 (calc) | 17.3 (calc) | 9.4 (37) |
| $Cu^{++}(aq)$ | 15.5±0.5 (36) | 15.4 (36) | -26.3 (53) |
| $Cu_2O$ | -36.4±1.5 (51) | -41.8±1.5 (51) | 24.1 (36) |
| CuO | -31.7±2.0 (51) | -38.3±2.0 (51) | 10.4 (36) |
| CuS | -11.63±5.5 (51) | -11.61±1.5 (51) | 15.9 (19) |
| Cu2S | -20.84±1.5 (51) | -19.48±1.0 (51) | 28.9 (19) |
| $Cu(OH)_2$ | -85.3 (36) | -106.1 (36) | 16.1 (calc) |
| $CuSO_4$ | -158.2 (19) | -184.0 (19) | 27.1 (19) |
| $S_2(g)$ | 19.13±1.0 (51) | 30.84±1.0 (51) | |
| S (rh) | 0 (19) | 0 (19) | 7.62 (19) |
| $S^=(aq)$ | 22.1 (19) | 8.56 (19) | -6.4 (19) |
| $H_2S$ | -7.91±0.7 (51) | -4.82±0.6 (51) | 49.15 (19) |
| $H_2S(aq)$ | -6.54 (19) | -9.4 (19) | 29.2 (19) |
| $HS^-(aq)$ | 3.01 (19) | -4.22 (19) | 14.6 (19) |
| $HSO_4^-$ | -179.9 (19) | -211.7 (19) | 30.3 (19) |
| $H_2SO_4$ | -177.3 (19) | -216.9 (19) | 4.1 (19) |
| $SO_4^=$ | -177.3 (19) | -216.9 (19) | 4.1 (19) |
| $Ag_2S$ | -9.44±1.0 (51) | -7.55±1.0 (51) | 34.8 (19) |
| ZnS (sph) | -47.4 (19) | -48.5 (19) | 13.8 (19) |
| FeS (pyrr) | -23.08±1.0 (51) | -22.4±1.0 (51) | 16.1 (19) |
| $Ni_3S_2$ | -47.97±5.0 (51) | -47.66±4.0 (51) | |
| NiS | -21.14±2.5 (51) | -21.68±2.5 (51) | |
| PbS | -22.34±1.5 (51) | -22.28±1.0 (51) | 21.8 (19) |
| SnS | -17.94±1.5 (51) | -18.4±1.5 (51) | 23.6 (19) |
| $SnS_2$ | -38.07±5.0 (51) | -39.96±5.0 (51) | |
| $Ag^+(aq)$ | 18.43 (19) | 25.31 (19) | 17.67 (19) |
| $Zn^{++}(aq)$ | -35.18 (19) | -36.43 (19) | -25.45 (19) |
| $Fe^{++}$ | -20.30 (19) | -21.0 (19) | -27.1 (19) |
| $Ni^{++}$ | -11.53 (19) | -15.3 (19) | |
| $Pb^{++}$ | -5.81 (19) | 0.39 (19) | 5.1 (19) |
| $Sn^{++}(aq)$ | -6.275 (19) | -2.39 (19) | -5.9 (19) |
| $Sn^{+4}(aq)$ | 0.650 (19) | | |

(References in brackets)

TABLE C-II

Calculated Half Cell Potentials

| | Electrode Reaction | Potential, V | V° | Deviation, + |
|---|---|---|---|---|
| 1 | $Cu_2S \rightarrow 2Cu^{++} + S + 4e^-$ | $0.563 + 0.0295 \log a_{Cu^{++}}$ | 0.563 | 0.027 |
| 2 | $Cu_2S \rightarrow 2Cu^{+} + S + 2e^-$ | $0.965 + 0.0591 \log a_{Cu^{+}}$ | 0.965 | 0.061 |
| 3 | $Cu_2S \rightarrow CuS + Cu^{++} + 2e^-$ | $0.535 + 0.0295 \log a_{Cu^{++}}$ | 0.535 | 0.130 |
| 4 | $Cu_2S \rightarrow CuS + Cu^{+} + e^-$ | $0.913 + 0.0591 \log a_{Cu^{+}}$ | 0.913 | 0.267 |
| 5 | $Cu_2S + 4H_2O \rightarrow 2Cu^{++} + HSO_4^- + 7H^+ + 10e^-$ | $0.428 + 0.0118 \log a_{Cu^{++}} - 0.0414$ pH | | |
| 6 | $Cu_2S + 4H_2O \rightarrow 2Cu^{++} + SO_4^{=} + 8H^+ + 10e^-$ | $0.440 + 0.0118 \log a_{Cu^{++}} - 0.0472$ pH | | |
| 7 | $2Cu_2S + H_2O \rightarrow Cu_2O + 2CuS + 2H^+ + 2e^-$ | $0.840 - 0.0591$ pH | | |
| 8 | $Cu_2S + 2H_2O \rightarrow Cu(OH)_2 + CuS + 2H^+ + 2e^-$ | $0.807 - 0.0591$ pH | | |
| 9 | $CuS \rightarrow Cu^{++} + S + 2e^-$ | $0.588 + 0.0295 \log a_{Cu^{++}}$ | 0.588 | 0.130 |
| 10 | $CuS \rightarrow Cu^{+} + S + e^-$ | $1.018 + 0.0591 \log a_{Cu^{+}}$ | 1.018 | 0.267 |
| 11 | $CuS + 4H_2O \rightarrow Cu^{++} + HSO_4^- + 7H^+ + 8e^-$ | $0.401 + 0.0074 \log a_{Cu^{++}} - 0.0517$ pH | | |
| 12 | $CuS + 4H_2O \rightarrow Cu^{++} + SO_4^{=} + 8H^+ + 8e^-$ | $0.415 + 0.0074 \log a_{Cu^{++}} - 0.0591$ pH | | |
| 13 | $CuS + 2H_2O \rightarrow Cu(OH)_2 + S + 2H^+ + 2e^-$ | $0.860 - 0.0591$ pH | | |
| 14 | $2CuS + H_2O \rightarrow CuO + Cu^{++} + 2S + 2H^+ + 4e^-$ | $0.690 - 0.0295$ pH | | |
| 15 | $Cu^{++} + 2H_2O \rightleftharpoons Cu(OH)_2 + 2H^+$ | $\log a_{Cu^{++}} + 2pH = 9.2$ | | |
| 16 | $2Cu^{+} \rightleftharpoons Cu^{++} + Cu$ | $K_{eq.} = 1 \times 10^6$ | | |

TABLE C-II (cont'd)

| | Electrode Reaction | Potential, V | V° | Deviation, ± |
|---|---|---|---|---|
| 17 | $Cu \rightarrow Cu^{++} + 2e^-$ | $0.336 + 0.0296 \log a_{Cu^{++}}$ | 0.336 | 0.008 |
| 18 | $Cu \rightarrow Cu^{+} + e^-$ | $0.513 + 0.0591 \log a_{Cu^{+}}$ | 0.513 | 0.028 |
| 19 | $SO_4^{=} + H^+ \rightleftharpoons HSO_4^-$ | pH = 1.9 ($a_{HSO_4^-} = a_{SO_4^=}$) | | |
| 20 | $H_2S(aq) \rightleftharpoons HS^- + H^+$ | pH = 7 ($a_{H_2S} = a_{HS^-}$) | | |
| 21 | $S + 4H_2O \rightarrow SO_4^- + 7H^+ + 6e^-$ | $0.339 - 0.069$ pH | | |
| 22 | $Ag_2S \rightarrow Ag^+ + S + 2e$ | $1.002 + 0.0591 \log a_{Ag^+}$ | 1.002 | |
| 23 | $Ag_2S \rightarrow AgS + Ag^+ + e$ | | | |
| 24 | $AgS \rightarrow Ag^+ + S + E$ | | | |
| 25 | $Ni_3S_2 \rightarrow 3Ni^{++} + 2S + 6e^-$ | $0.0962 - 0.0295 \log a_{Ni^{++}}$ | 0.0962 | |
| 26 | $Ni_3S_2 \rightarrow 2NiS + Ni^{++} + 2e^-$ | $-0.126 + 0.0295 \log a_{Ni^{++}}$ | -0.126 | |
| 27 | $NiS \rightarrow Ni^{++} + S + 2e^-$ | $0.209 + 0.0295 \log a_{Ni^{++}}$ | 0.209 | |
| 28 | $PbS \rightarrow Pb^{++} + S + 2e^-$ | $0.358 + 0.0295 \log a_{Pb^{++}}$ | 0.358 | |
| 29 | $ZnS$ (sphalerite) $\rightarrow Zn^{++} + S + 2e^-$ | $0.265 + 0.0295 \log a_{Zn^{++}}$ | 0.265 | |
| 30 | $FeS_2 \rightarrow Fe^{++} + 2S + 2e^-$ | $0.060 + 0.0295 \log a_{Fe^{++}}$ | 0.060 | |
| 31 | $SnS_2 \rightarrow Sn^{++} + 2S + 2e^-$ | $0.688 + 0.0295 \log a_{Sn^{++}}$ | 0.688 | |
| 32 | $SnS \rightarrow Sn^{++} + S + 2e$ | $0.253 + 0.0295 \log a_{Sn^{++}}$ | 0.253 | |
| 33 | $Sn^{++} \rightarrow Sn^{+4} + 2e^-$ | $0.150 + 0.0295 \log \frac{a_{Sn^{+4}}}{a_{Sn^{++}}}$ | 0.150 | |

# APPENDIX D

## Electrode Potentials of Metal Sulphides

Noddack and Wrabetz[11,12] and Sato[47] measured the potential of $Ag_2S$, $Cu_2S$, CuS, PbS, FeS, $FeS_2$ and ZnS electrodes in acid and basic solutions. Their results are summarized in Table D-I and discussed briefly.

TABLE D-I

Electrode Potentials for Several Sulphides

| Electrode | Expected Reaction | Measured Potential, V | | Calculated Potential, V |
|---|---|---|---|---|
| | | Noddack & Wrabetz | Sato | |
| $Cu_2S$ | $Cu_2S \longrightarrow CuS + Cu^{++} + 2e^-$ | 0.474 | 0.504 | 0.535 |
| CuS | $CuS \longrightarrow Cu^{++} + S + 2e$ | 0.58 | 0.567 | 0.588 |
| PbS | $PbS \longrightarrow Pb^{++} + S + 2e$ | 0.367 | 0.370 | 0.354 |
| $Ag_2S$ | $Ag_2S \longrightarrow 2Ag^+ + S + 2e$ | 0.812 | 0.82 | 1.002 |
| ZnS | ZnS(sphalerite) $\longrightarrow$ $Zn^{++} + S + 2e$ | 0.5 | | 0.26 |
| $FeS_2$ | $FeS_2 \longrightarrow Fe^{++} + S_2 + 2e$ | 0.5 | 0.7 | 0.757 |

Sato explained the discrepancy between the measured and calculated values for the potential of the $Ag_2S$ electrode by assuming that a two-stage reaction was taking place, viz:

$$Ag_2S \longrightarrow AgS + Ag^+ + e$$

$$AgS \longrightarrow Ag^+ + e^-$$

No value of the free energy of AgS is available, so this mechanism cannot be substantiated. However, if the measured value of 0.82 V is assumed to be the electrode potential for the reaction

$$Ag_2S \longrightarrow AgS + Ag^+ + e^-,$$

then the free energy of formation of AgS can be calculated to be - 8,890 cal/mole.

The measurements of Noddack and Wrabetz demonstrated the influence of the Ag/S ratio on the electrode potential. For example, for an electrode with Ag/S = 1.99, V° = 0.812 V; and for an electrode with Ag/S = 1.84, V° = 0.853 V. Sato does not reveal the stoichiometry of his electrode, but it likely had Ag/S = 2, approximately.

Although nickel sulphide is oxidized electrochemically on a commercial scale, no electrode potentials were noted in the literature. Renzoni et al[1] characterize the nickel sulphide oxidation by the following overall reaction:

$$Ni_3S_2 \longrightarrow 3\ Ni^{++} + 25° + 6e \qquad V° = 0.417\ V$$

Several other nickel sulphides are known to exist[52], so it is likely, in view of the oxidation mechanism suggested for other polyvalent sulphides (e.g. copper sulphide), that several stepwise processes are involved in the oxidation of $Ni_3S_2$. One possible mechanism is:

$$Ni_3S_2 \longrightarrow Ni^{++} + 2\ NiS + 2e \qquad V° = -0.126\ V$$

$$NiS \longrightarrow Ni^{++} + S° + 2e^- \qquad V° = 0.209\ V$$

An electrochemical series for the sulphides has been established based on the above information, and is shown in Table D-II.

TABLE D-II

Tentative Electrochemical Series for Some Metal Sulphides

| Electrode | Electrode Potential, V° |
|---|---|
| $Ag_2S$ | 0.82 |
| $FeS_2$ | 0.7 |
| CuS | 0.59 |
| $Cu_2S$ | 0.53 |
| PbS | 0.35 |
| ZnS | 0.26 |
| NiS | 0.21 |
| $Ni_3S_2$ | -0.13 |

# APPENDIX E

## Potentials at the Electrode-Solution Interface

### Electrode Potential

Metal sulphide electrodes generally follow the Nernst relationship in acid solution. When Nernstian behaviour is followed by an electrode, a definite potential is established between the electrode and solution, fully predictable from a knowledge of the activities and free energies of the electrode and solution constituents. Quite often this potential is called the reversible potential, but this term should only be used when the electrode reaction in question is truly reversible, i.e. when a small change in potential from one side of the reversible potential to the other will reverse the direction of the electrode reaction. A more general and universally applicable term for the potential established between an electrode and a solution is the rest potential; this term appears most appropriate when considering compound electrodes such as the sulphides because a truly reversible reaction involving the compound and its components is highly improbable in acid solutions because of the stability of the sulphur atoms or molecules. It presupposes only that the several reactions occurring spontaneously at the electrode surface are in electrical balance.

### Electrode-Solution Interface

A detailed and sophisticated discussion of the electrode-solution interface has been presented by Parsons[29]. When an electrode is placed in an aqueous solution, there is a redistribution of the electrical charge associated with the particles which come

from the bulk of the two phases (electrode and solution) to form the interface or interfacial layer. This redistribution of charge forms a region which is called the double layer. The species which are involved in the electrochemical reaction across the double layer exist in energy wells: in the electrode, the well is produced by the influence of the other atoms and ions in the metal (or sulphide, or oxide) lattice; in the solution, the well is produced by the influence of water molecules (hydrated species) or of other ions (complexed species). It is useful to picture an energy well in the electrode moving close enough to an energy well in the solution so that the energy barrier between the two wells is small enough that a transfer of species between the two wells can be effected. Depending on the relative depth of the two energy wells, the transfer can be either anodic or cathodic, but there is a tendency for the two transfers to move towards a balanced state where the anodic and cathodic processes are virtually balanced. The potential and the current flow across the energy barrier are called the rest potential and the exchange current respectively.

Butler[30] calculated that several electron volts are required to lift bare unsolvated cations from their energy wells in the metal lattice, and energies of the same order of magnitude would likely be necessary to remove a bare unsolvated cation from a sulphide lattice. Also, Butler[30] and Eley and Evans[31] calculated that several electron volts are required to lift a bare cation out of its hydration sheath. However, the transfer of a cation from a metal (or metal compound) lattice to the solution requires only

about 5 mV potential. Thus the energy wells in the two phases must be very close together. The water molecules are touching the electrode and may be even bonded to it by adsorption bonds even stronger than their own intermolecular bonds[29].

Overpotential

When an additional electrode is added to the solution to complete the galvanic cell, and an external potential is applied, the rest condition is altered to a net cathodic or anodic condition depending on the direction of the applied potential. The additional potential across the double layer constitutes a driving force for electrochemical reactions at the electrode, and tends to increase the current flow through the cell. A new term, the overpotential, is defined.

The overpotential at a certain current density is the difference between the measured potential and the previously established rest potential; if the overpotential is represented by $\omega$, then

$$\omega = \phi_i - \phi_0$$

where $\phi_i$ and $\phi_0$ are the half-cell potentials at net current densities i and zero respectively. Various types of overpotential have been distinguished (see, for example, reference 13, pp 395-398), but the three important types are ohmic, concentration, and activation overpotential.

An ohmic overpotential is developed when a film is formed on the electrode and sets up a resistance to the passage of current

across it; the film can be an oxide or sulphide, sulphur or some other substance. If the current strength is i and the film resistance R, then the ohmic overpotential will be iR. Values of several hundred volts are possible for the ohmic overpotential[41].

A concentration overpotential is caused by the existence of a difference in concentration of ions between the electrode-solution interface or double layer and the bulk of the solution. As the potential of the electrode is related to the ionic concentration in the double layer, and the potential measured by a reference electrode is related to the bulk ionic concentration, serious errors would be introduced in potential measurement if the concentration overpotential was not recognized and either allowed for or removed. The phenomenon of concentration overpotential forms the basis of polorography and polarographic analysis.

The third type, activation overpotential, is developed when a reacting species encounters a barrier which it must climb before it can proceed along the reaction path; thus the activation overpotential is related to the energy of activation (i.e. the energy "height" of the barrier) and, if carefully determined, can provide both the identification of the rate-determining step and the rate of reaction in activation-controlled electrochemical reactions. For the simplest case, the activation barrier exists between two adjacent energy wells, one in the electrode and the other in the solution. If a physical description is to be attached to the activation barrier in this case, it is easy to picture the barrier being established by the redistribution of the electrical

charges of the various bulk phase species when the two phases are brought in contact with one another.

The success of experiments to determine the activation overpotential depends on the minimization of ohmic and concentration overpotentials. The procedures necessary to minimize the unwanted overpotentials are described in the section on Experimental Procedure.

# APPENDIX F

## Kinetic Relationships for Activation Controlled Electrode Reactions

A generalized cathodic reaction has been chosen to illustrate the development of electrode kinetic relationships. The discussion is essentially a simplification of that presented by Bockris[14]. The overall reaction is represented by equation (F1):

$$\text{Reactants} + ne^- \longrightarrow \text{Products} \qquad \ldots\ldots(F1)$$

Likely several steps are involved in transferring the reacting species across the solution-electrode interface and placing them on the cathode, but normally one of these steps will have a larger free energy barrier than the others and thus will control the reaction rate. Figure F1 illustrates a hypothetical energy profile along a reaction co-ordinate. The highest peak represents the rate-controlling barrier, and unless the reacting species attain this free energy level, they cannot pass on to become products. When a representative point of a reaction exists at this peak (albeit for an exceedingly short time), it is called the activated complex of the reacting species.

The activities of the reacting species at point x (just before the highest barrier) are related to the activities of the species in the initial state at point 1, and if the two states are considered to be in equilibrium, the relationship can be described thus:

$$(\prod a_r)_x = (\prod a_r)_1 \exp\left(\frac{-\Delta F°1 \rightarrow x}{RT}\right) \qquad \ldots\ldots(F2)$$

where $(\prod a_r)_1$ and $(\prod a_r)_x$ are the products of the activities of the

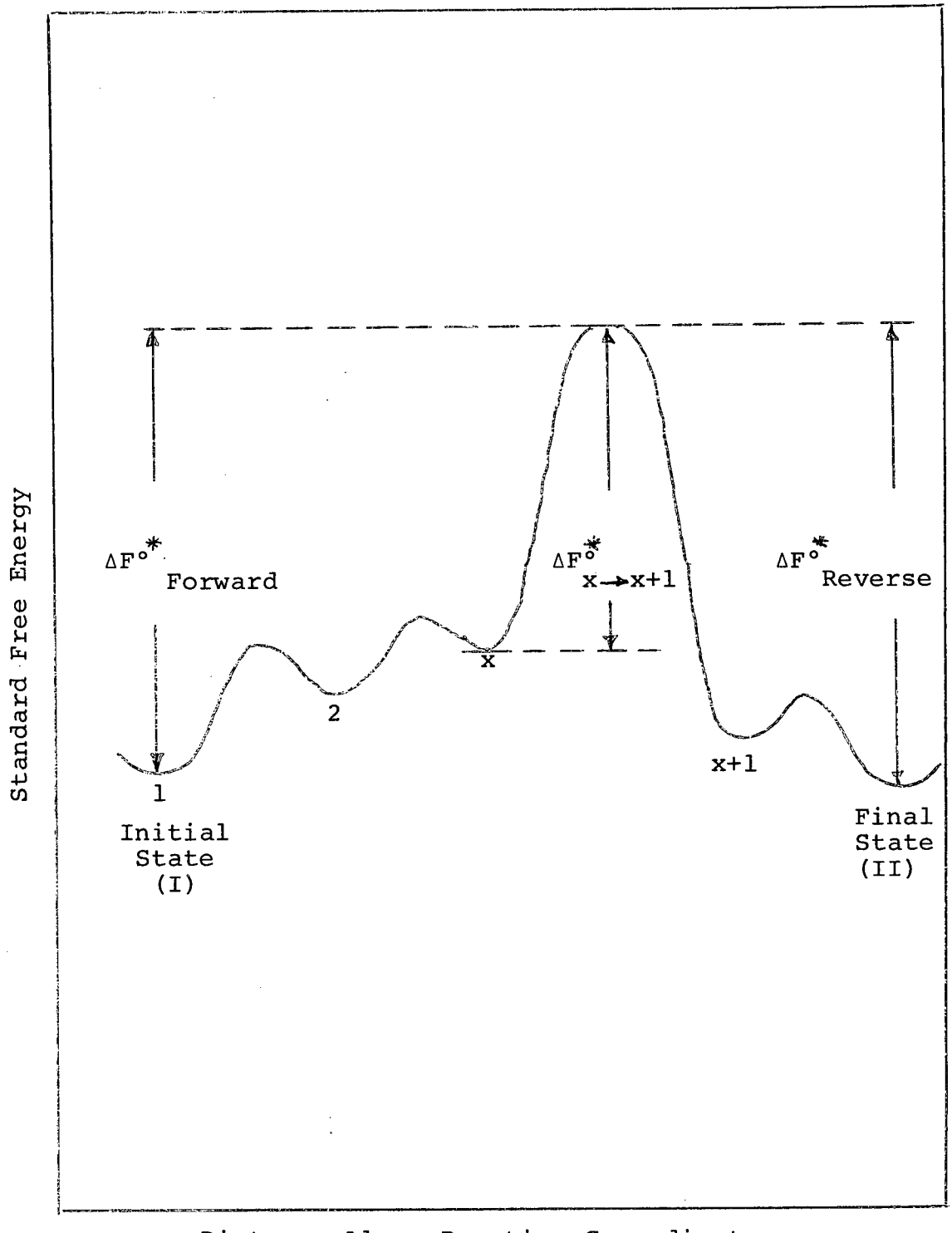


Figure F1. Reaction Path and Energy Barriers for a Series of Consecutive Reactions

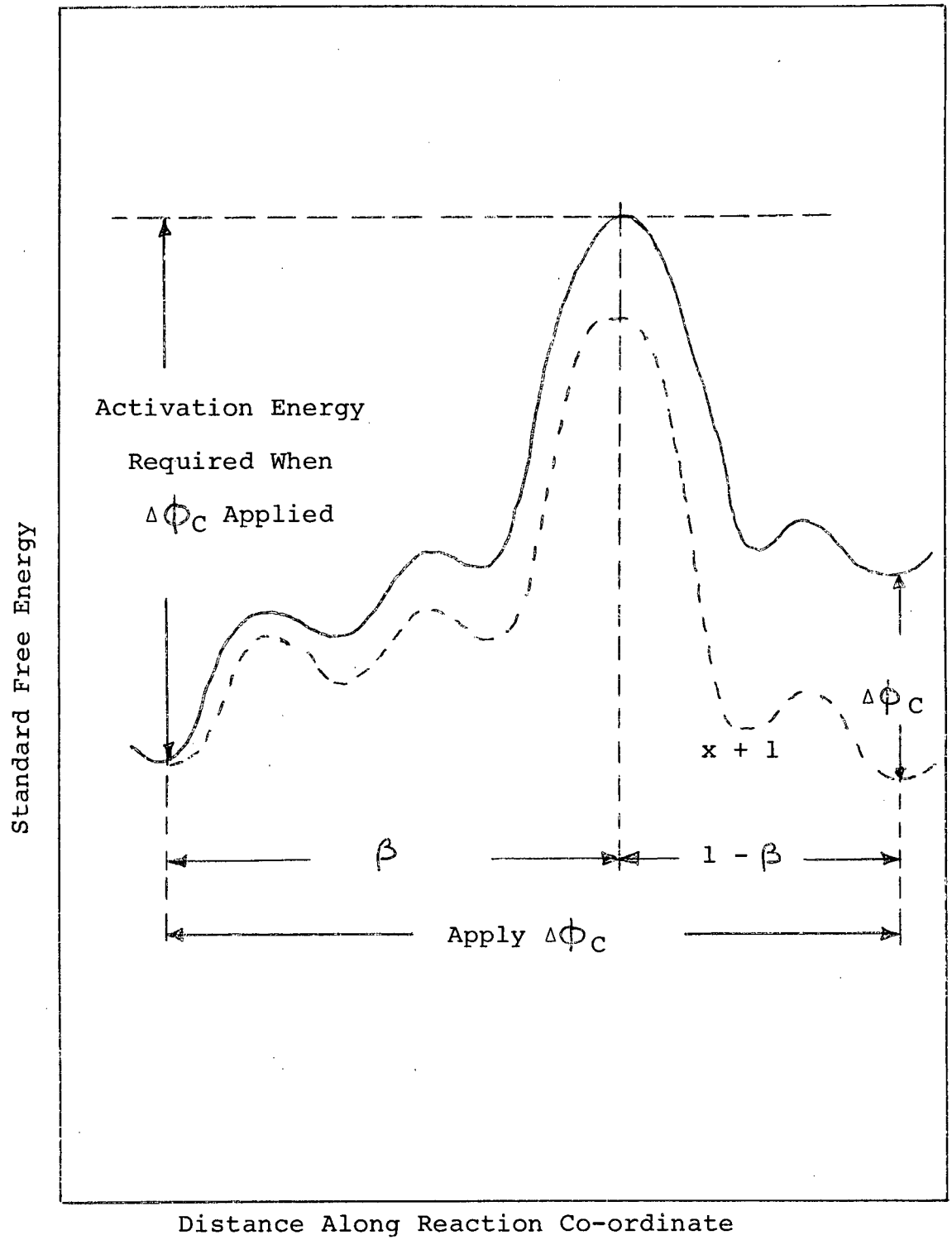


Figure F2. Reaction Path and Energy Barriers when Potential $\Delta\phi_C$ Applied

reactants in the initial and xth states respectively, (each activity being raised to the power equivalent to the number of moles involved in the reaction) and $\Delta F°_{1 \rightarrow x}$ is the free energy change during transition from 1 to x. The forward velocity of the reaction across the rate-controlling barrier can be expressed conveniently as

$$\vec{v} = (\Pi a_r)_x \vec{k} \qquad \text{.....(F3)}$$

where k, the specific rate constant, is given by:

$$\vec{k} = K \frac{kT}{h} \exp \left( -\frac{\Delta F°^{\ddagger}_{x \rightarrow x+1}}{RT} \right) \qquad \text{.....(F4)}$$

In equation (F4), K is the transmission coefficient (i.e. the fraction of the species reaching the activated complex state which proceeds to products), and k, T, h and R have their usual physical significance.

The current density is a convenient measure of the velocity of electrode reactions and is related to the velocity by

$$\vec{i} = \vec{v} \lambda \mathcal{F} \qquad \text{.....(F5)}$$

where $\lambda$ is the number of electrons necessary so that one act of the rate-determining step can occur and $\mathcal{F}$ is the Faraday constant. Furthermore, if the rate determining step occurs $\nu$ times when the overall reaction (F1) occurs once, then:

$$\lambda = \frac{n}{\nu} \qquad \text{.....(F6)}$$

If a positive potential difference $\Delta\phi_C$ is applied between the final and initial state of the reaction (Figure F-2), the flow of reactants over the rate-determining barrier is retarded. The applied potential difference $\Delta\phi_C$ increases $\Delta F°^{\ddagger}_{x \rightarrow x+1}$ by an amount

$\beta\lambda 7\Delta\phi_C$, where $\beta\Delta\phi_C$ is the portion of the applied potential which retarded the passage of species to the activated complex state; it is not necessary to account for the potential difference beyond the activated state because work done on the system after it has passed the activated state does not alter the reaction velocity. The term $\beta$ describes the symmetry of the energy barrier in relation to the overall reaction distances. By combining (F2), (F3), (F4) and (F5), the following relationship for the forward current density is obtained:

$$\vec{i} = K\lambda 7 \frac{kT}{h} (\Pi a_r)_1 \exp\left[-\frac{\Delta F^\circ_{1\rightarrow x} + \Delta F^{\circ\ddagger}_{x\rightarrow x+1} + \beta\lambda\Delta\phi_C 7}{RT}\right] \qquad .....(F7)$$

or, on simplification:

$$\vec{i} = B_C(\Pi a_r)_1 \exp\left[-\frac{\Delta F^{\circ\ddagger}_C + \beta\lambda\Delta\phi_C 7}{RT}\right] \qquad .....(F8)$$

By a similar argument, the relationship for the reverse reaction, i.e. anodic dissolution, is obtained:

$$\overleftarrow{i} = B_A(\Pi a_r)_2 \exp\left[-\frac{F^{\circ\ddagger}_A - (1-\beta)\lambda\Delta\phi_C 7}{RT}\right] \qquad .....(F9)$$

As a basis for developing potential-current density relationships, the equilibrium or rest situation (i.e. no net current flow) is first considered:

$$\vec{i} - \overleftarrow{i} = 0 \quad ; \quad \vec{i} = \overleftarrow{i} = i_0 \qquad .....(F10)$$

where $i_0$ is the exchange current. The overpotential $\omega$ can be defined as:

$$\omega = \Delta\phi_C - \Delta\phi_O \qquad .....(F11)$$

where $\Delta\phi_O$ is the potential when $i = i_0$. When equation (F8), (F9), (F10) and (F11) are combined, the following are obtained:

$$\overrightarrow{i} = i_0 \exp\left[-\frac{\beta\lambda\omega\mathcal{F}}{RT}\right] \qquad .....(F12)$$

$$\overleftarrow{i} = i_0 \exp\left[\frac{(1-\beta)\lambda\omega\mathcal{F}}{RT}\right] \qquad .....(F13)$$

$$i_C = i_0 \exp\left[-\frac{\beta\lambda\omega\mathcal{F}}{RT}\right] - \exp\left[\frac{(1-\beta)\lambda\omega\mathcal{F}}{RT}\right] \qquad .....(F14)$$

and similarly,

$$i_A = i_0 \exp\left[\frac{(1-\beta)\lambda\omega\mathcal{F}}{RT}\right] - \exp\left[-\frac{\beta\lambda\omega\mathcal{F}}{RT}\right] \qquad .....(F15)$$

where $i_C$ and $i_A$ are the resultant current densities for cathodic precipitation and anodic dissolution respectively under an applied potential .

Several simplifications of equation (F15) are important. If $\omega$ is quite large (i.e. if $\omega > \frac{2.303\ RT}{\lambda\mathcal{F}}$)* then

$$i_A = i_0 \exp\frac{(1-\beta)\lambda\omega\mathcal{F}}{RT} \qquad .....(F16)$$

This can be rewritten as

$$\omega = -\frac{RT}{(1-\beta)\lambda\mathcal{F}} \ln i_0 + \frac{RT}{(1-\beta)\lambda\mathcal{F}} \ln i_A \qquad .....(F17)$$

or

$$\omega = A + B \ln i_A \qquad .....(F18)$$

Equation (F18) is the most common relationship in electrode kinetics, the so-called "Tafel" line. Now if $\omega$ is small (i.e. if $\omega < \frac{2.303\ RT}{\lambda\mathcal{F}}$), then equation (F15), on expansion of the exponentials, becomes

$$i_A = i_0 \frac{\lambda\mathcal{F}}{RT}\omega \qquad .....(F19)$$

or

$$\omega = \frac{RT}{i_0\lambda\mathcal{F}} i_A \qquad .....(F20)$$

---

* $\frac{2.303\ RT}{\lambda\mathcal{F}} \approx$ 20-30 mV if $\lambda = 2$ at 25°C.

Hurlen[34,35] has developed a method for determining the standard heat of activation of certain electrode reactions. The standard heat of activation ($\Delta H_o^*$) for any reaction is defined as the change in standard heat content (on the hydrogen scale) of the reaction system when going from its initial to its activated state:

$$\Delta H_o^* = H_o^* - H_o^{(i)} \qquad .....(F21)$$

In order to define the standard heat content of the activated state in terms consistent with those usually used for the reactant, the frequency factor $\nu$ must be introduced:

$$\Delta H_o^* = H_o^* - \frac{1}{\nu} H_o^{(i)} \qquad .....(F22)$$

Further, if it is assumed the same frequency factor applied to both the forward and reverse reaction across the activation barrier, then

$$\overrightarrow{\Delta H_o^*} - \overleftarrow{\Delta H_o^*} = \frac{1}{\nu} \overrightarrow{\Delta H_o} \qquad .....(F23)$$

At this point the standard exchange current, $J_0$, is defined:

$$J_0 = i_0 \left[ (\Pi a_r)^{1-\beta} (\Pi a_p)^{\beta} \right]^{-1/\nu} \qquad .....(F24)$$

Utilizing this definition of $J_0$, the relationships expressed in equations (F7), (F8), (F9), (F14) and (F15) can be described by an Arrhenius equation of the following type:

$$\log \frac{J_0}{T} = C - \frac{\beta n \mathcal{F} \Delta\phi}{2.303 \nu RT} - \frac{\Delta H_o^*}{2.303\ RT} \qquad .....(F25)$$

The term n represents the number of electrons consumed during one act of the overall reaction (positive for cathodic and negative for anodic reactions). Constant C consists mainly of temperature independent constants and includes the standard entropy of activation and the activity coefficient of the activated complex; both of which are here considered temperature independent. The Galvani potential $\Delta\phi$ cannot be determined experimentally, but if the

reaction is symmetrical, i.e. the forward and reverse reaction across the activation barrier are the same, then the term in equation (F25) containing $\Delta\phi$ will be equal in magnitude but opposite in sign for the forward and reverse reaction. Then

$$2 \log (J_0/T) = \overrightarrow{C} + \overrightarrow{C} - \frac{\overrightarrow{\Delta H_o}^* + \overleftarrow{\Delta H_o}^*}{2.303\ RT} \qquad .....(F26)$$

If equation (F26) is differentiated with respect to 1/T and combined with equation (F23), then

$$\Delta H_o^* = -2.303\ R\ \frac{d \log(J_0/T)}{d\ (1/T)} + \frac{1}{2}\ \Delta H_o \qquad .....(F27)$$

Thus if the activation barrier is symmetrical, i.e. if $\beta = 1/2$, and if the assumptions inherent in the above derivation are acceptable, it is then possible to determine the standard heat of activation of that electrode reaction*.

---

* It is tacitly assumed that the transmission coefficient K is the same for both forward and reverse transfer across the activation barrier.

# APPENDIX G

## Activity Coefficients in $CuSO_4$-$H_2SO_4$ Solutions

One of the difficulties in determining electrode potentials in mixed solutions is the lack of good values for the activity coefficients of the various ionic species. Argersinger[25] derived relationships for determining the activity coefficients of electrolytes in mixed aqueous solution from electromotive force data. Holland and Bonner[26] investigated $CuSO_4$-$H_2SO_4$ mixed aqueous solutions and obtained a series of electromotive force measurements; however, they did not extend their work to include an application of Argersinger's procedure to determine mean activity coefficients for the individual electrolytes. Such an extension is attempted here.

Consider the galvanic cell

$$P \left| \; \upsilon^+ A_{\upsilon}^- \; (m_1) \right\| \; Q_{\beta}^+ \; A_{\beta}^- \; (m_2) \left| \; Q \right.$$

where $P_{\upsilon^+} A_{\upsilon^-}$ and $Q_{\beta^+} A_{\beta^-}$ are the two electrolytes in aqueous solution. The cell potential $\mathcal{E}$ is defined by

$$\mathcal{E} = \mathcal{E}^\circ + \frac{RT}{\mathcal{F}} \ln \frac{a_1^{1/K_1}}{a_2^{1/K_2}} \qquad \text{.....(G1)}$$

where $a_1$ = activity of $P_{\upsilon^+} A_{\upsilon^-}$

$a_2$ = activity of $Q_{\beta^+} A_{\beta^-}$

$K_1 = (\upsilon^+)(Z_P) = (\upsilon^-)(Z_A)$

$K_2 = (\beta^+)(Z_Q) = (\beta^-)(Z_A)$

$Z_Q$, $Z_P$, $Z_A$ = charges on ions

Then, using the procedure of Argersinger[25], the following relationships can be derived:

$$\ln \frac{\gamma_1}{\gamma_1^\circ} = \frac{Z_P Z_A}{Z_P + Z_A} \int_y^1 \left[ (1-y) \frac{\partial G}{\partial y} + N \frac{\partial G}{\partial N} \right] dy \qquad \text{.....(G2)}$$

$$\ln \frac{\gamma_2}{\gamma_2^\circ} \quad \frac{Z_Q Z_A}{Z_Q + Z_A} \int_o^y \left[ y \frac{\partial G}{\partial y} - N \frac{\partial G}{\partial N} \right] dy \qquad \text{.....(G3)}$$

where $\gamma_1$ = mean activity coefficient of component 1.

$\gamma_1^\circ$ = activity coefficient of component 1 in its pure solution in the solvent (i.e. water) at the same value of N as in the mixed solution.

$$N = \frac{1000}{M_{solvent}} \left[ \frac{n_1 K_1 + n_2 K_2}{n_{solvent}} \right]$$

$= m_1 K_1 + m_2 K_2$ for water, where $m_1$ and $m_2$ are molalities.

$$y = \frac{m_1 K_1}{m_1 K_1 + m_2 K_2}$$

$$G = - \ln \frac{\gamma_1^{\left(\frac{1}{Z_P} + \frac{1}{Z_A}\right)}}{\gamma_2^{\left(\frac{1}{Z_Q} + \frac{1}{Z_A}\right)}}$$

The data of Holland and Bonner[26], derived from electromotive force measurements, are in the form of values of $\frac{\gamma^3 H_2SO_4}{\gamma^2 CuSO_4}$ for various values of $\frac{m_{H^+}}{m_{Cu^{++}}}$ and $\mu$, the total ionic strength. It is necessary to relate these measurements to the terms of equations (2) and (3).

If $H_2SO_4$ and $CuSO_4$ are solutions 1 and 2 respectively, then $Z_P = 1$, $Z_A = 2$ and $Z_Q = 2$. Now

$$G = - \ln \frac{\gamma_1^{1/1 + 1/2}}{\gamma_2^{1/2 + 1/2}} = - 1/2 \ln \frac{\gamma_1^3}{\gamma_2^2}$$

$$G = - 1/2 \ln \frac{\gamma^3 H_2SO_4}{\gamma^2 CuSO_4} \qquad \text{.....(G4)}$$

Also,

$$y = \frac{m_1 K_1}{m_1 K_1 + m_2 K_2}$$

or

$$y = \frac{2m_1}{2m_1 + 2m_2} = \frac{m_1}{m_1 + m_2}$$

$$y = \frac{m_{H_2SO_4}}{m_{H_2SO_4} + m_{CuSO_4}}$$

But

$$m_{H^+} = 2m_{H_2SO_4}$$

and

$$m_{SO_4^{=}} = 1/2\ m_{H^+} + m_{Cu^{++}}$$

Therefore

$$y = \frac{1/2\ m_{H^+}}{1/2\ m_{H^+} + m_{Cu^{++}}} = \frac{m_{H^+}}{m_{H^+} + 2m_{Cu^{++}}}$$

If

$$\frac{m_{H^+}}{m_{Cu^{++}}} = R \qquad \text{.....(G5)}$$

then

$$y = \frac{R}{R + 2} \qquad \text{.....(G6)}$$

Also

$$N = m_1 K_1 + m_2 K_2$$

$$= 2\ (m_1 + m_2)$$

$$= 2\ (m_{H_2SO_4} + m_{CuSO_4})$$

$$N = m_{H^+} + 2m_{Cu^{++}} \qquad \text{.....(G7)}$$

The total ionic strength, $\mu$, is defined as

$$= 1/2 \sum_i C_i Z_i^2$$

For this solution

$$\mu = \frac{3}{2} m_{H^+} + 4m_{Cu^{++}} \qquad \text{.....(G8)}$$

By combining equations (G5), (G7) and (G8), the following is obtained:

$$N = 2\mu \frac{R + 2}{3R + 8} \qquad \text{.....(G9)}$$

Thus equations (G4), (G6) and (G9) provide the relationships necessary to use the data of Holland and Bonner[26] in equations (G2) and (G3).

The values of G, y and N are compiled in Table G-I. The important relations needed for equations (G2) and (G3) are $\left(\frac{\partial G}{\partial N}\right)_y$ and $\left(\frac{\partial G}{\partial y}\right)_N$. Figure G-1 is a plot of G vs N at constant y, and is characterized by considerable irregularity. In fact $(\partial G/\partial N)_y$ is first a large positive value, then zero, then a large negative value, then zero, and finally above N = 0.5, a positive value again. These data should be analysed by the Gibbs-Duhem integration technique to give a reasonable precision over the wide range of N. For the region above N = 0.5 however, the slope $(\partial G/\partial N)_y$ is reasonably uniform, so as an approximation, the average value of these slopes has been used. It is realized that considerable error is probably introduced by this approximation, but there is a possibility that the regions of large positive and negative slope will in effect largely cancel each other in a Gibbs-Duhem integration. From the approximation, the following value is obtained.

$$\left(\frac{\partial G}{\partial N}\right)_y = -0.040 \quad \text{for} \quad N > 0.5 \qquad \text{.....(G10)}$$

Further treatment of the data gives:

$$\left(\frac{\partial G}{\partial y}\right)_N = 0.282 \quad \text{for} \quad N > 0.5 \qquad \text{.....(G11)}$$

Equation (G3) is integrated:

$$\ln \frac{\gamma_2}{\gamma_2^\circ} = 1/2 \frac{\partial G}{\partial y} y^2 - N \frac{\partial G}{\partial N} y \qquad .....(G12)$$

Calculated values of $\gamma_{CuSO_4}$ for a number of $CuSO_4$-$H_2SO_4$ solutions are shown in Table G-II. These values are compared in Table G-III with those determined by Hurlen[39] from electrode potential measurements. The values of $\gamma_{CuSO_4}$ are plotted against $\mu$, the ionic strength, in Figure G-2. The difference between the values of Hurlen and those calculated herein is equivalent to a difference in the electrode potential of about 0.005 V (for n = 2). Hurlen's values depend on some assumed values of liquid junction potentials, so they probably have a limited accuracy. The present values are probably even less dependable because of the approximation used in their calculation, but they should be applicable for values of N greater than 0.5 and for values of y greater than 0.7. For N = 0.5 and y = 0.7, the concentrations are: $Cu^{++}$, 0.075 M, and $H^+$, 0.35 M. Thus, the calculated activity coefficients are probably most applicable to solutions of relatively high concentration (say $Cu^{++} > 0.01$ M, $H^+ > 0.1$ M). The use of the calculated values of $\gamma_{CuSO_4}$ gave a satisfactory resolution of the electrode potential measurements in 0.1 M $CuSO_4$ - 0.1 M $H_2SO_4$ solutions obtained in this work. The calculated values of $\gamma_{CuSO_4}$ are probably not absolutely correct, but the use of the approximate calculation rather than a proper integration probably develops a constant error.

TABLE G-I

Determination of G, y and N from Data of Holland and Bonner[26]

| $\frac{m_{H^+}}{m_{Cu^{++}}}$ | $\frac{\gamma^3 H_2SO_4}{\gamma^2 CuSO_4}$ | G | y | $\mu$ | $\frac{R+2}{3R+8}$ | N |
|---|---|---|---|---|---|---|
| 7.178 | 1.795 | -0.293 | 0.783 | 1.319 | 0.311 | 0.820 |
| | 1.726 | -0.273 | | 0.897 | | 0.558 |
| | 1.698 | -0.265 | | 0.509 | | 0.316 |
| | 1.686 | -0.262 | | 0.2522 | | 0.157 |
| | 1.547 | -0.218 | | 0.1280 | | 0.0797 |
| | 1.535 | -0.218 | | 0.0638 | | 0.397 |
| | 1.304 | -0.133 | | 0.0307 | | 0.0191 |
| | 0.932 | +0.035 | | 0.0154 | | 0.00959 |
| 5.435 | 1.712 | -0.269 | 0.732 | 1.359 | 0.306 | 0.832 |
| | 1.672 | -0.257 | | 0.926 | | 0.567 |
| | 1.634 | -0.246 | | 0.522 | | 0.319 |
| | 1.596 | -0.234 | | 0.2637 | | 0.161 |
| | 1.647 | -0.250 | | 0.1314 | | 0.0805 |
| | 1.610 | -0.238 | | 0.0634 | | 0.0388 |
| | 1.442 | -0.183 | | 0.0312 | | 0.0191 |
| | 1.009 | - | | 0.0159 | | 0.00974 |
| 3.294 | 1.634 | -0.245 | 0.623 | 1.309 | 0.297 | 0.777 |
| | 1.572 | -0.226 | | 0.878 | | 0.521 |
| | 1.596 | -0.234 | | 0.500 | | 0.297 |
| | 1.633 | -0.246 | | 0.319 | | 0.189 |
| | 1.523 | -0.211 | | 0.1409 | | 0.0836 |
| | 1.670 | -0.257 | | 0.0634 | | 0.0376 |
| | 1.476 | -0.195 | | 0.0312 | | 0.0185 |
| | 1.168 | -0.0778 | | 0.0159 | | 0.00945 |
| 1.660 | 1.466 | -0.192 | 0.454 | 1.334 | 0.282 | 0.752 |
| | 1.442 | -0.183 | | 0.878 | | 0.495 |
| | 1.488 | -0.189 | | 0.520 | | 0.293 |
| | 1.547 | -0.218 | | 0.2353 | | 0.133 |
| | 1.634 | -0.246 | | 0.1303 | | 0.0735 |
| | 1.692 | -0.263 | | 0.0652 | | 0.0368 |
| | 1.547 | -0.218 | | 0.0317 | | 0.0179 |
| | 1.254 | -0.113 | | 0.0159 | | 0.00898 |
| 1.026 | 1.376 | -0.160 | 0.339 | 1.477 | 0.273 | 0.806 |
| | 1.355 | -0.152 | | 0.010 | | 0.552 |
| | 1.420 | -0.175 | | 0.576 | | 0.315 |
| | 1.523 | -0.210 | | 0.2874 | | 0.157 |
| | 1.672 | -0.258 | | 0.1441 | | 0.0788 |
| | 1.698 | -0.265 | | 0.0717 | | 0.0392 |
| | 1.622 | -0.242 | | 0.0351 | | 0.0192 |
| | 1.314 | -0.137 | | 0.0139 | | 0.0076 |
| 0.361 | 1.313 | -0.136 | 0.265 | 1.401 | 0.260 | 0.730 |
| | 1.295 | -0.129 | | 0.950 | | 0.494 |
| | 1.356 | -0.152 | | 0.689 | | 0.358 |
| | 1.477 | -0.195 | | 0.344 | | 0.179 |
| | 1.600 | -0.254 | | 0.1374 | | 0.0715 |
| | 1.713 | -0.270 | | 0.0693 | | 0.0360 |
| | 1.573 | -0.227 | | 0.0275 | | 0.0143 |
| | 1.400 | -0.168 | | 0.0160 | | 0.00835 |

TABLE G-II

Computation of $\gamma_{CuSO_4}$

| M $CuSO_4$, $= m_2$ | $M_{H_2SO_4} = m_1$ | $\mu$ = ionic strength | R | N | Equivalent Solution $m_{CuSO_4}$ | $\gamma_{CuSO_4}$* $= \gamma_2^\circ$ | y | $\ln \frac{\gamma_2}{\gamma_2^\circ}$ | $= \gamma_2 = \gamma_{CuSO_4}$ |
|---|---|---|---|---|---|---|---|---|---|
| 0.01 | 0.05 | 0.19 | 10 | 0.12 | 0.06 | 0.210 | 0.833 | -0.09384 | 0.191 |
| 0.03 | 0.05 | 0.27 | 3.33 | 0.16 | 0.08 | 0.175 | 0.625 | -0.05108 | 0.166 |
| 0.10 | 0.05 | 0.55 | 1.0 | 0.3 | 0.15 | 0.121 | 0.333 | -0.01167 | 0.120 |
| 0.30 | 0.05 | 1.35 | 0.33 | 0.7 | 0.35 | 0.076 | 0.143 | +0.00111 | 0.077 |
| 0.10 | 0.10 | 0.7 | 2.0 | 0.4 | 0.2 | 0.104 | 0.50 | -0.02725 | 0.099 |

* values from reference 16

TABLE G-III

Mean Ionic Activity Coefficient of $CuSO_4$ in some $CuSO_4$-$H_2SO_4$ Solutions

| Molarity+ $CuSO_4$ | Molarity+ $H_2SO_4$ | Ionic Strength = $\mu$ | $\gamma_{CuSO_4}$ at 25°C | $CuSO_4$ after Hurlen[39] at 20°C | $CuSO_4$ after Hurlen[39] 25°C* |
|---|---|---|---|---|---|
| 0.01 | 0.05 | 0.19 | 0.191 | 0.280 | 0.286 |
| 0.03 | 0.05 | 0.27 | 0.166 | 0.224 | 0.230 |
| 0.10 | 0.05 | 0.55 | 0.120 | 0.161 | 0.166 |
| 0.30 | 0.05 | 1.35 | 0.077 | 0.129 | 0.133 |
| 0.10 | 0.10 | 0.7 | 0.099 | | (0.150)N |

+ Molarity $\simeq$ Molality at the concentrations

* $\log \gamma 25 = \log \gamma 20$ (293/298)

N Estimated from Figure G-2

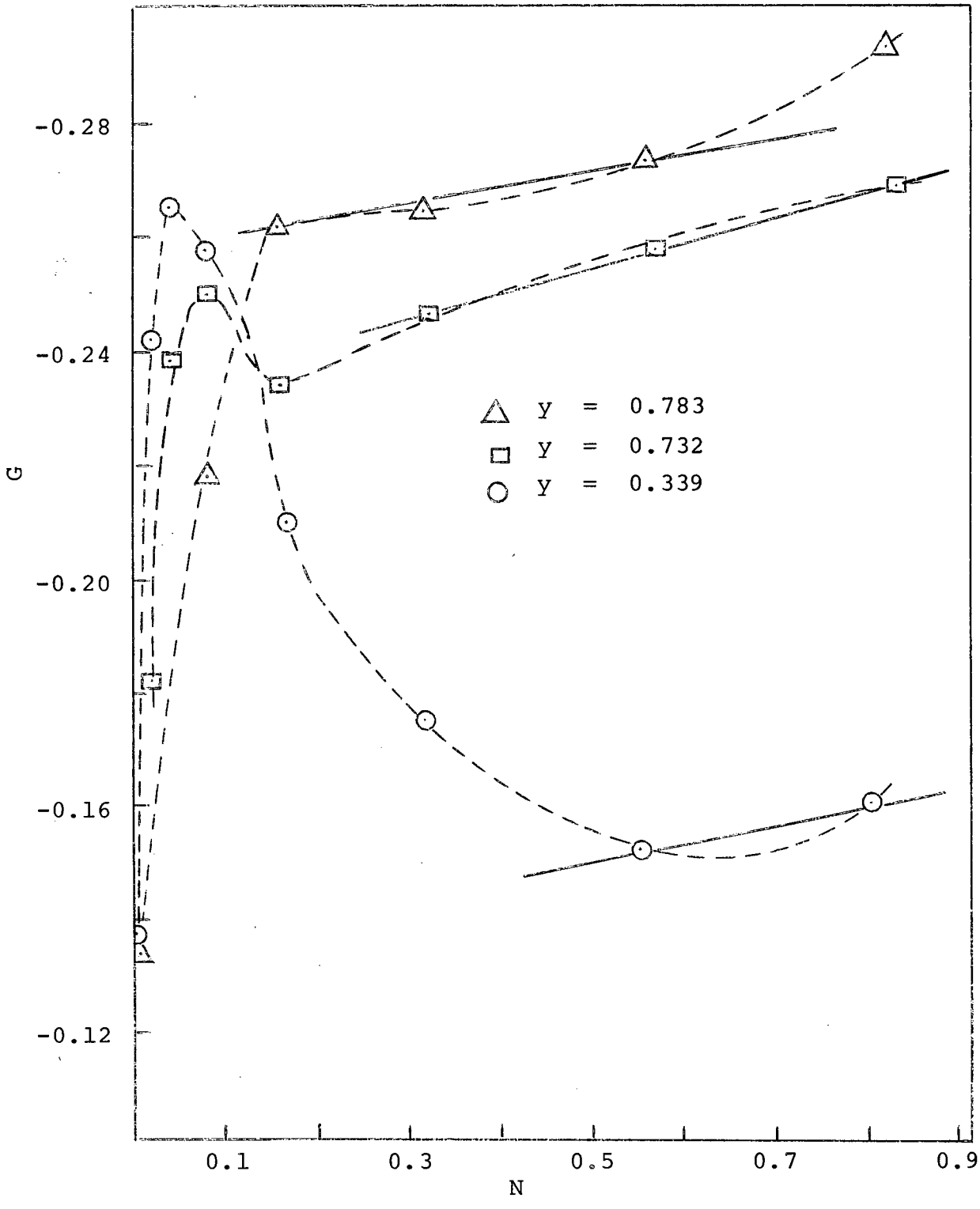


Figure G1. Plot of G vrs. N from Data of Table G-I

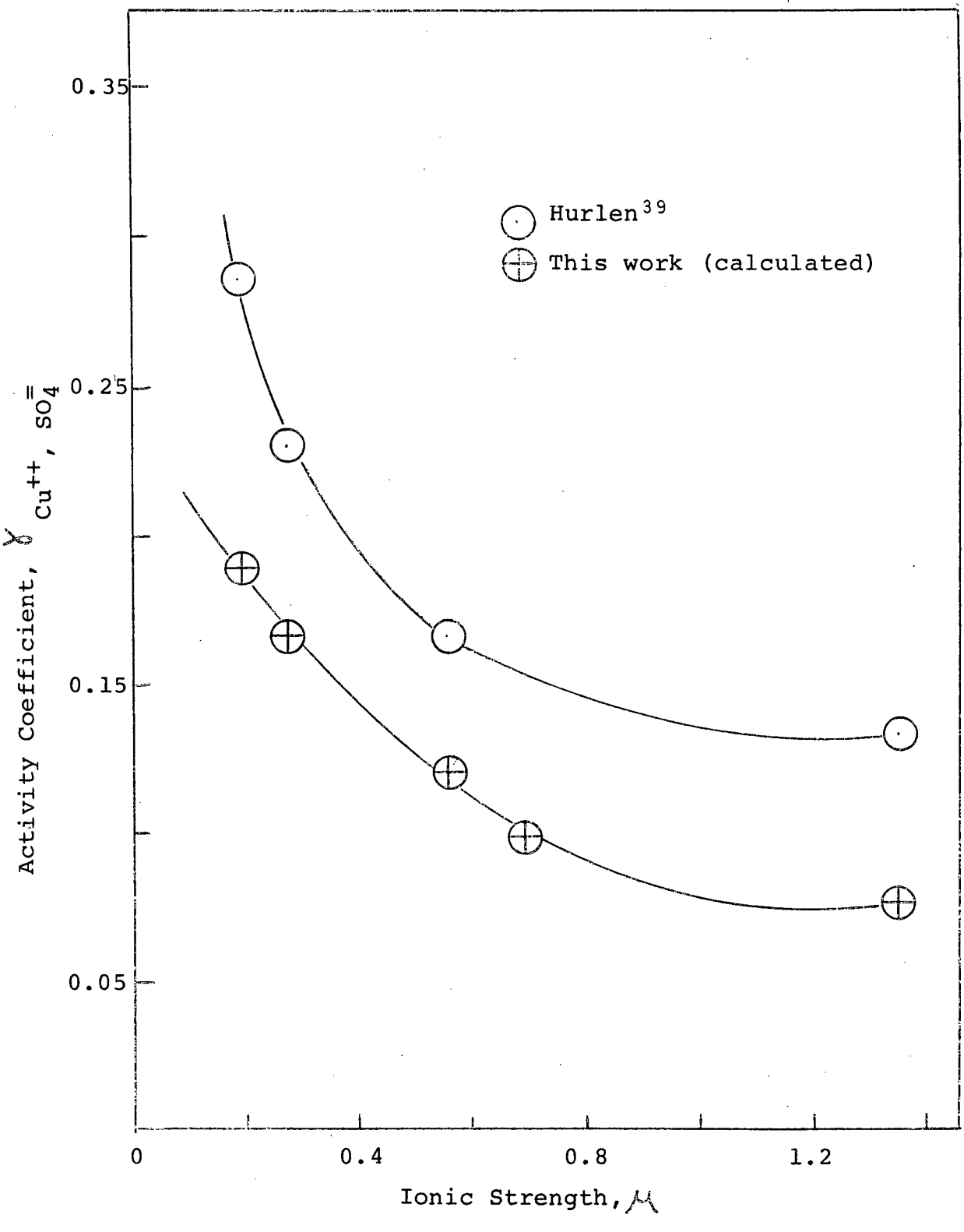


Figure G2. Mean Activity Coefficient as a Function of Ionic Strength for $CuSO_4$ in $H_2SO_4$ Solutions at 25° C

# APPENDIX H

## X-ray Powder Patterns

Debye-Schirrer photographs were obtained for the cuprous sulphide electrode, analytical grade CuS, and an anodic oxidation reaction product (Figure H1).

The three principal lines on the cuprous sulphide picture (Figure H1-a) are equivalent to d spacings of 2.28, 1.88 and 1.79 Å; the accepted values (x-ray data card 12-227) are 2.40, 1.97 and 1.88 Å. The agreement is not unreasonable, especially with the small camera. It is concluded that the electrode is cuprous sulphide, probably the rhombohedral $\alpha$ - chalcocite.

The photographs for the analytical grade CuS and the reaction product (Figures H1-b and H1-c) are very similar, so it is concluded that the reaction product is probably CuS.

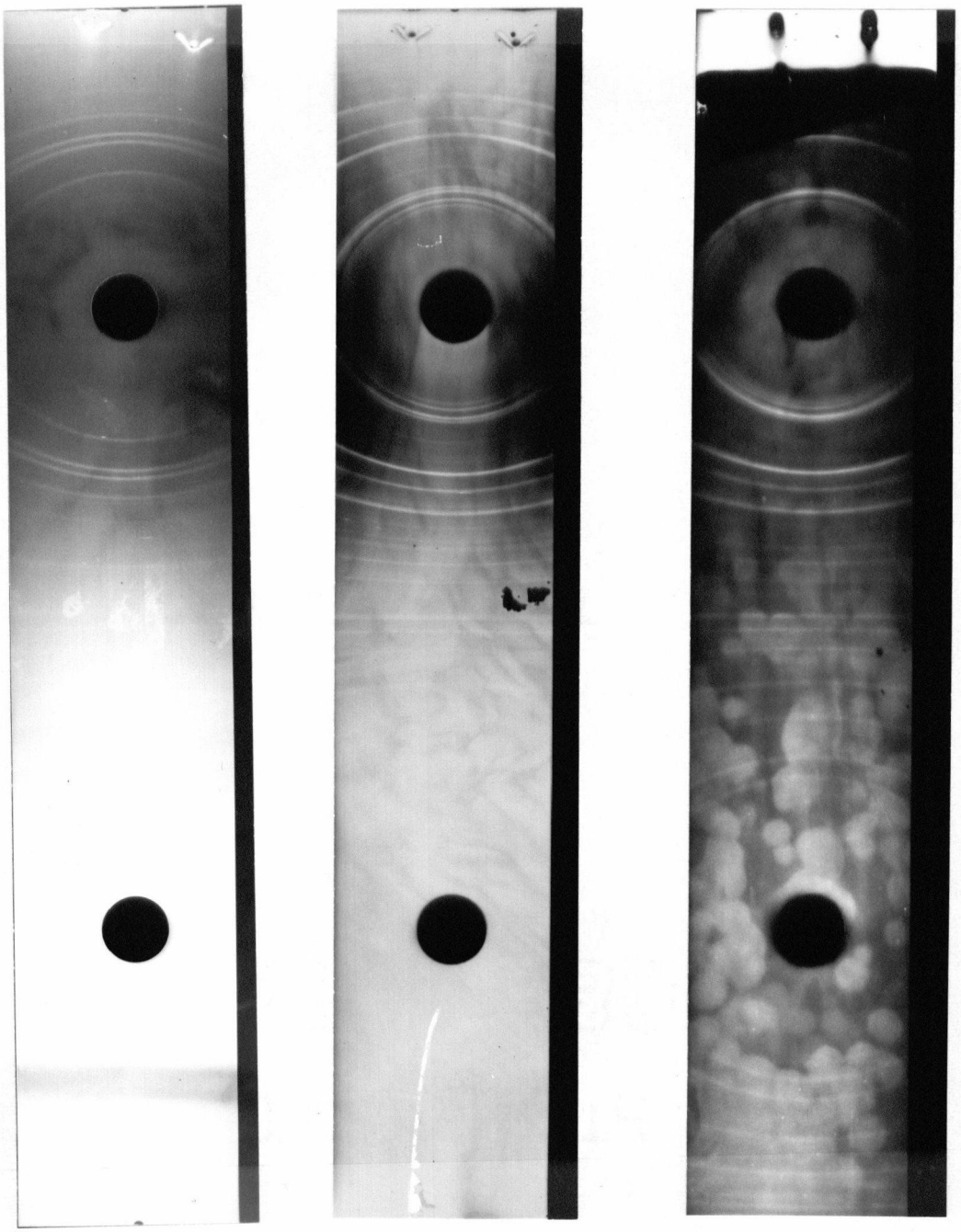

(a) (b) (c)

Figure H1. X-ray Powder Pictures: (a) $Cu_2S$, (b) CuS and (c) Reaction Product